

Efficient Inference of Macrophylogenies: Insights from the Avian Tree of Life

MIN ZHAO^{1,2,*}, GREGORY THOM^{3,4,†}, BRANT C. FAIRCLOTH^{3,4}, MICHAEL J. ANDERSEN⁵, F. KEITH BARKER⁶, BRETT W. BENZ⁷, MICHAEL J. BRAUN^{8,9}, GUSTAVO A. BRAVO^{10,11}, ROBB T. BRUMFIELD^{12,13}, R. TERRY CHESSE^{12,13}, ELIZABETH P. DERRYBERRY¹⁴, TRAVIS C. GLENN¹⁵, MICHAEL G. HARVEY¹⁶, PETER A. HOSNER¹⁷, TYLER S. IMFELD¹⁸, LEO JOSEPH¹⁹, JOSEPH D. MANTHEY²⁰, JOHN E. MCCORMACK²¹, JENNA M. MCCULLOUGH^{5,22}, ROBERT G. MOYLE²³, CARL H. OLIVEROS⁴, NOOR D. WHITE CARREIRO²⁴, KEVIN WINKER²⁵, DANIEL J. FIELD^{26,27}, DANIEL T. KSEPKA^{28,29}, EDWARD L. BRAUN^{1,*}, REBECCA T. KIMBALL^{1,*}, AND BRIAN TILSTON SMITH^{29,*}

¹Department of Biology, University of Florida, 876 Newell Dr, Gainesville, FL 32611, USA

²Department of Biological Sciences, Virginia Tech, 926 West Campus Dr, Blacksburg, VA 24061, USA

³Museum of Natural Science, Louisiana State University, 119 Dalrymple Dr, Baton Rouge, LA 70802, USA

⁴Department of Biological Sciences, Louisiana State University, 202 Life Sciences Bldg, Baton Rouge, LA 70803, USA

⁵Department of Biology and Museum of Southwestern Biology, University of New Mexico, 219 Yale Blvd NE, Albuquerque, NM 87131, USA

⁶Bell Museum of Natural History and Department of Ecology, Evolution and Behavior, University of Minnesota, 1987 Upper Buford Circle, St. Paul, MN 55108, USA

⁷Department of Ecology and Evolutionary Biology and Museum of Zoology, University of Michigan, 3600 Varsity Dr, Ann Arbor, MI 48108, USA

⁸Department of Vertebrate Zoology, National Museum of Natural History, Smithsonian Institution, 1000 Constitution Ave, Washington, DC 20560, USA

⁹Department of Biology and Biological Sciences Graduate Program, University of Maryland, 1247 Biology-Psychology Building, College Park, MD 20742, USA

¹⁰Center for Biological Collections and Species Management, Instituto Alexander von Humboldt, Cra. 8 #152, Villa de Leyva, Boyacá, Colombia

¹¹Museum of Comparative Zoology & Department of Organismic and Evolutionary Biology, Harvard University, 26 Oxford Street, Cambridge, MA 02138, USA

¹²U.S. Geological Survey, Eastern Ecological Science Center, 12100 Beech Forest Road, Laurel, MD 20708, USA

¹³Department of Vertebrate Zoology, National Museum of Natural History, Smithsonian Institution, PO Box 37012, Washington, DC 20013, USA

¹⁴Department of Ecology and Evolutionary Biology, University of Tennessee, 1416 Circle Dr, Knoxville, TN 37996, USA

¹⁵Department of Environmental Health Science and Institute of Bioinformatics, University of Georgia, 150 East Green Street, Athens, GA 30602, USA

¹⁶Department of Biological Sciences and Biodiversity Collections, The University of Texas at El Paso, 500 W University Avenue, El Paso, TX 79968, USA

¹⁷Natural History Museum of Denmark and Center for Global Mountain Biodiversity, University of Copenhagen, Universitetsparken 15, DK-2100 Copenhagen, Denmark

¹⁸Department of Biology, Xavier University, 3800 Victory Parkway, Cincinnati, OH 45207, USA

¹⁹Australian National Wildlife Collection, CSIRO National Research Collections Australia, Canberra, ACT 2602, Australia

²⁰Department of Biological Sciences, Texas Tech University, 2901 Main St, Lubbock, TX 79409, USA

²¹Moore Laboratory of Zoology, Occidental College, 1600 Campus Road, Los Angeles, CA 90041, USA

²²Department of Biology, University of Kentucky, 195 Hugeluet Dr, Lexington, KY 40508, USA

²³Department of Ecology and Evolutionary Biology and Biodiversity Institute, University of Kansas, 1200 Sunnyside Avenue, Lawrence, KS 66045, USA

²⁴Biological Imaging Core, National Eye Institute, National Institutes of Health, 9000 Rockville Pike, Bethesda, MD 20892, USA

²⁵University of Alaska Museum, 907 Yukon Drive, Fairbanks, AK 99775, USA

²⁶Department of Earth Sciences, University of Cambridge, Downing St, Cambridge CB2 3EQ, UK

²⁷Museum of Zoology, University of Cambridge, Downing Pl, Cambridge CB2 3EJ, UK

²⁸Bruce Museum, 1 Museum Dr, Greenwich, CT 06830, USA

²⁹Department of Ornithology, American Museum of Natural History, Central Park West at 79th Street, New York, NY 10024, USA

*Correspondence to be sent to: Min Zhao, Department of Biology, University of Florida, Gainesville, FL 32611, USA; E-mail: balaenazhao@gmail.com; Edward L. Braun, Department of Biology, University of Florida, Gainesville, FL 32611, USA; ebraun68@ufl.edu; Rebecca T. Kimball, Department of Biology, University of Florida, Gainesville, FL 32611, USA; rkimball@ufl.edu; Brian Tilston Smith, Department of Ornithology, American Museum of Natural History, Central Park West at 79th Street, New York, NY 10024, USA; briantilstonsmith@gmail.com

†Contributed equally.

Received 16 February 2025; reviews returned 15 September 2025; accepted 31 October 2025

Associate Editor: Robert Thomson

Abstract.—The exponential growth of molecular sequence data over the past decade has enabled the construction of numerous clade-specific phylogenies encompassing hundreds or thousands of taxa. These independent studies often include overlapping data, presenting a unique opportunity to build macrophylogenies (phylogenies sampling >1000 taxa) for entire classes across the Tree of Life. However, the inference of large trees remains constrained by logistical, computational, and methodological challenges. The Avian Tree of Life provides an ideal model for evaluating strategies to robustly infer

macrophylogenies from intersecting data sets derived from smaller studies. In this study, we leveraged a comprehensive resource of sequence capture data sets to evaluate the phylogenetic accuracy and computational costs of four methodological approaches: (1) supermatrix approaches using concatenation, including the “fast” maximum likelihood (ML) methods, (2) filtering data sets to reduce heterogeneity, (3) supertree estimation based on published phylogenomic trees, and (4) a “divide-and-conquer” strategy, wherein smaller ML trees were estimated and subsequently combined using a supertree approach. Additionally, we examined the impact of these methods on divergence time estimation using a data set that includes newly vetted fossil calibrations for the Avian Tree of Life. Our findings highlight the advantages of recently developed fast tree search approaches initiated with parsimony starting trees, which offer a reasonable compromise between computational efficiency and phylogenetic accuracy, facilitating inference of macrophylogenies. [Macrophylogeny; phylogenomics; supermatrix; supertree; ultraconserved elements; birds.]

Completing the Tree of Life remains a significant bottleneck to addressing a wide range of questions in comparative biology (Cracraft and Donoghue 2004). Advances in sequencing technologies (reviewed by McCormack, Hird, et al. 2013), computational methods (e.g., Kozlov et al. 2019), and user-friendly bioinformatic pipelines (e.g., Faircloth 2016) have made the production and analysis of phylogenomic data sets involving hundreds of taxa increasingly routine. However, scaling these techniques to data sets with thousands of loci and thousands of taxa presents substantial logistical, computational, and methodological challenges (Delsuc et al. 2005; Philippe et al. 2011; Kapli et al. 2020). The construction of such “macrophylogenies” (Title and Rabosky 2017) often relies on combining independently produced data sets, which frequently have limited overlap and substantial missing data (Sanderson et al. 2010).

Past attempts to infer macrophylogenies from independently produced data sets typically used two general approaches: supermatrix and supertree methods. Supermatrix methods infer phylogenies directly from orthologous loci, often compiled from multiple studies. However, these methods are negatively affected by large amounts of missing data (Driskell et al. 2004; Philippe et al. 2004; Goloboff et al. 2009; Hosner et al. 2016) and varying standards of data quality (Philippe et al. 2011). Analyses of supermatrices are also vulnerable to common issues in phylogenetic analyses, such as alignment errors (Ogden and Rosenberg 2006) and the inclusion of non-orthologous sequences (Koonin 2005), which are often exacerbated in supermatrices due to the heterogeneous nature of the data. Additionally, supermatrix methods face escalating computational demands that increase nonlinearly (Bader et al. 2006) as both the width (number of sites) and height (number of taxa) of the matrix expand (Delsuc et al. 2005). Some challenges, such as data quality and alignment issues, can be mitigated to an extent by analyzing multiple data sets filtered to remove “noise” in different ways and comparing the results (Kuhl et al. 2021). However, this approach is limited by the significant computational costs of performing multiple analyses on large data sets. Supertree methods, by contrast, generate phylogenies by combining existing tree topologies (Sanderson et al. 1998; Bininda-Emonds 2004; Cotton and Wilkinson 2009). These methods are more computationally efficient and can effectively incorporate trees built with heterogeneous data (Liu et al.

2001; Hinchliff et al. 2015; Redelings and Holder 2017). However, most supertree methods cannot directly estimate meaningful branch lengths. Despite the strengths and limitations of these methods, rigorous comparisons of the ability of supermatrix and supertree methods to estimate macrophylogenies using phylogenomic data remain rare. This gap largely reflects the limited availability of large-scale genomic data sets for most taxonomic groups.

Class Aves (birds) is one taxonomic group with sufficient data to perform these types of comparative analyses. As the most species-rich terrestrial vertebrate group, with 11,140 species recognized (Gill et al. 2023), birds have received extensive attention from phylogenetic systematists (e.g., Hackett et al. 2008; Jetz et al. 2012; McCormack, Harvey, et al. 2013; Jarvis et al. 2014; Burleigh et al. 2015; Prum et al. 2015; Moyle et al. 2016; Reddy et al. 2017; Oliveros et al. 2019; Harvey et al. 2020; Stiller et al. 2024). Many relationships among birds are now strongly corroborated across studies, providing a reliable framework for evaluating the accuracy of alternative approaches to estimate macrophylogenies. Another advantage of birds as a model system is the partial standardization of phylogenomic data collection through the widespread use of targeted enrichment of nuclear loci, such as ultraconserved elements (UCEs *sensu* Faircloth et al. 2012). Over a quarter of all avian species now have UCE data available (see below). These data have been used to resolve phylogenetic relationships among birds at both deep (e.g., McCormack, Harvey, et al. 2013; Jarvis et al. 2014; Oliveros et al. 2019; Harvey et al. 2020) and shallow (e.g., Smith et al. 2014; Winker et al. 2018) timescales. Most UCE studies of birds target a large, uniform set of loci (uce-5k-probe-set, available from <https://github.com/faircloth-lab/uce-probe-sets>; e.g., Sun et al. 2014). Some studies instead use a smaller, nested subset of these loci (uce-2.5k-probe-set) that is sometimes combined with exons commonly used in avian phylogenetics (e.g., Smith et al. 2014; Harvey et al. 2020). Although these data sets exhibit some heterogeneity—stemming from the use of different bait sets and variability in the quality of input DNA templates—extensive overlap facilitates integration into a single comprehensive data set.

In this study, we use phylogenomic data from birds to empirically evaluate the accuracy and computational cost of alternative tree estimation approaches. By as-

sembling orthologous UCE loci from the primary literature, we aim to better understand the factors influencing the estimation of macrophylogenies. Specifically, we address the following questions: (1) Do computationally efficient methods, such as “fast” maximum likelihood (ML) estimation, supertrees, or a divide-and-conquer strategy that combines many small trees using a supertree method, recover similar numbers of expected relationships corroborated in prior studies as traditional ML methods? (2) Does filtering data sets to reduce size and heterogeneity result in topologies that recover fewer expected clades, and how does it affect compute time? (3) Does the use of different methods, which may bias branch length estimation and produce distinct topologies, affect divergence time estimation? By combining phylogenomic data from independent studies, we constructed a large-scale avian phylogeny, encompassing 2756 ingroup taxa, 2 outgroup taxa, and 5121 loci. Our findings demonstrate that it is possible to infer an accurate macrophylogeny with moderate computational cost. Moreover, the strategies identified as most effective in this study are likely applicable to other taxonomic groups with sufficient phylogenomic data.

MATERIALS AND METHODS

Assembling the Phylogenomic data

We took multiple approaches to create a database of UCE loci from existing studies of birds. We downloaded much of the data as individual alignments from 22 phylogenomic studies (Zhang et al. 2014; Bryson et al. 2016; Hosner et al. 2016; McCormack et al. 2016; Manthey et al. 2016; Burga et al. 2017; Campillo et al. 2018; Andermann et al. 2019; Andersen et al. 2019; Everson et al. 2019; McCullough, Joseph, et al. 2019; McCullough, Moyle, et al. 2019; Oliveros et al. 2019; Sackton et al. 2019; White and Braun 2019; Harvey et al. 2020; Imfeld et al. 2020; Oliveros et al. 2020; Salter et al. 2020; Smith et al. 2023; Braun et al. 2024; for details, see [Supplementary Table S1](#) and [Supplementary Information](#)). We noticed that several studies had overlapping or nested taxon sampling. For example, Moyle et al. (2016) collected UCE data for 104 songbird species, and these data had all been included in a later study with broader taxon sampling (Oliveros et al. 2019). Therefore, we used the data set from Oliveros et al. (2019) for downstream analyses.

All studies targeted UCES as the main genetic markers (some also targeted a small number of legacy markers), and we preferentially downloaded alignments with as little filtering as possible (e.g., no missing data cut-offs). For studies where individual alignments were unavailable, we downloaded concatenated matrices and partition files, which we converted into alignments using the “split” function of AMAS (Borowiec 2016). Finally, we extracted UCES and 500-bp flanking sequences from genome assemblies available at NCBI (that were not under embargo; data downloaded on 14 October

2020) for species that were not represented by UCE sequences, following Tutorial III of PHYLUCES (Faircloth 2016) with the 5k probe set.

We processed the sequences to retain only one individual per species, according to the IOC World Bird List v13.1 (Gill et al. 2023). When multiple individuals of the same species were present in our alignments or the same sample was used in different studies, we arbitrarily selected the representative sample based on the alphabetical order of the studies ([Supplementary Table S1](#)). A few exceptions arose from taxonomic changes, occasionally causing minor duplication or inclusion of multiple subspecies representing the same species (see [Data Availability](#)). After verifying taxa, we performed sequence alignment with MAFFT (Katoh and Standley 2013) using default settings and the `-adjustdirection` option to correct for sequence orientation. Then, we filtered raw alignments with trimAl (Capella-Gutiérrez et al. 2009) using the “gappyout” method to remove sites based on the gap distribution within each alignment. We refer to these alignments as the “full” data set. We anticipated substantial heterogeneity in the original data sets used to generate our supermatrix. See [Supplementary Information](#) for how we evaluated data heterogeneity.

Filtering Loci and Subsetting Data Sets

To assess how different locus filtering schemes affect topology and computational cost, we created 27 filtered data sets by applying three filtering schemes serially to the full data set ([Fig. 1a](#)). First, to control for missing sequence data by taxon, that is, effects of partial sequences, or “type II” missing data (*sensu* Hosner et al. 2016), we prepared two data sets where we removed taxa from alignments when they were shorter than 50% or 75% of the longest sequence in the alignment for each locus ([Fig. 1a](#), Step I). Then we ran these two data sets, plus the full data set, through a second stage of filtering to control for gappyness by retaining alignment positions with at least 90%, 70%, and 50% occupancy ([Fig. 1a](#), Step II). This step helps to address potential issues with indel-induced alignment gaps (e.g., Dwivedi and Gadagkar 2009) and reduce heterogeneity that can occur at the ends of UCE alignments. Finally, for each of the nine data sets that resulted, we performed a third stage of filtering to control for taxon completeness, where we retained loci with at least 90% ($n = 2484$), 70% ($n = 1932$), and 50% ($n = 1380$) of the total number of taxa ([Fig. 1a](#), Step III). The last step helps to control for the effects of incomplete taxon sampling, that is, “type I” missing data (*sensu* Hosner et al. 2016). We concatenated each of these data sets using PHYLUCES (Faircloth 2016) prior to phylogenetic analysis.

For each filtered data set and the full data set, we averaged the individual-based summary statistics (see [Supplementary Information](#)) across all taxa sampled in that data set ([Supplementary Table S2](#)). To visually inspect if taxa were clustering by study, we performed

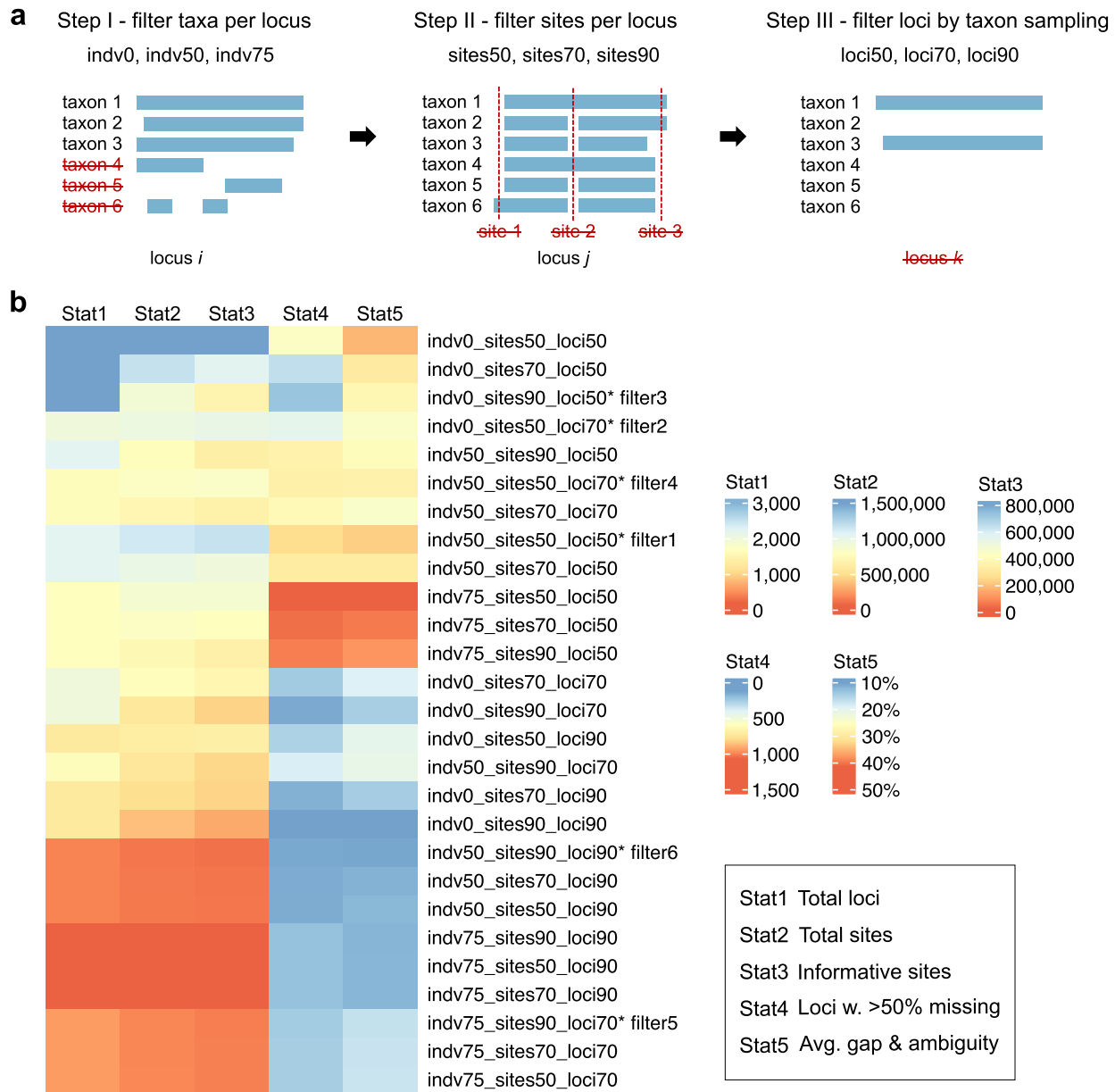


FIGURE 1. Filtering schemes and information content of different data sets. (a) We used a combination of three strategies to filter data sets. Step I. Indv refers to the removal of individual taxa with short sequences for specific loci: indv0 indicates that we did not conduct this filtering step; indv50 and indv75 indicate that sequences shorter than 50% and 75% of the longest sequence for that alignment were removed. Step II. Sites refers to the trimming of sites dominated by gaps and missing data: sites50 indicates that alignment columns where $\geq 50\%$ of taxa were gaps or missing are removed; sites70 and sites90 removed columns with $\geq 70\%$ or $\geq 90\%$ gaps or missing data, respectively. The percentage of taxa with gaps or missing data in a column reflects the number of taxa sampled for the locus of interest. Step III. Loci refers to the removal of poorly sampled loci: loci50, loci70, and loci90 indicate that loci are retained only if they are sampled for $\geq 50\%$, $\geq 70\%$, and $\geq 90\%$ (respectively) of taxa in the full data matrix. (b) Summary statistics (total number of loci, total number of sites, total number of parsimony informative sites, loci with $>50\%$ data missing, and average proportion of gaps and ambiguities ["-", "?", and "N"] across all loci) of the sequence alignments in all 27 filtered data sets. For missing data information (Stat4 and Stat5), hotter colors represent more missing data.

principal component analysis (PCA) using FactoMineR v1.34 (Lé et al. 2008) on individual-based summary statistics and plotted the first two principal components using ggplot2 v3.3.5.9 (Wickham 2011) in R (R Core Team 2023). We also used IQ-TREE2 (Nguyen et al. 2015) to compute locus-based summary statistics for each fil-

tered data set, that is, number of loci, total sites, parsimony informative sites, average gap and ambiguity across all loci, and loci with more than 50% missing data (Supplementary Table S3). We used ComplexHeatmap (Gu 2022) to plot the locus-based summary statistics for 27 filtered data sets (Fig. 1b).

Initial Data Exploration

Concatenated analyses.— We used the message passing interface (MPI) version of RAxML-NG v1.0.1 (Kozlov et al. 2019) to infer an ML phylogeny of the concatenated, full data set (Table 1, baseline). Because this data set was large, we ran two concurrent ML analyses that each used 800 CPUs—both used the GTR+R4 site rate substitution model, but one used parsimony to generate starting trees (MP starting trees) whereas the other used random starting trees. Because of the compute hours allocated to this project, we were only able to infer seven ML phylogenies using random starting trees and five ML phylogenies using MP starting trees for the RAxML-NG analysis. We selected the optimal tree as the one having the highest log-likelihood across the 12 analyses. We generated support values for the full data set by performing ML analysis on 10 standard bootstrap (Felsenstein 1985) replicates with the GTR+R4 model. We evaluated the bootstrap replicates for convergence using the `-bs-converge` option. We found that these replicates had converged, and we reconciled the “best” ML tree with the bootstrap replicates using RAxML-NG.

To explore a faster method for ML tree estimation, we used the `-fast` option in IQ-TREE v2.0.5 (Nguyen et al. 2015) with the GTR+G site rate substitution model (Table 1, strategy 1). We initially inferred phylogenies from the concatenated, full data set along with six filtered data sets that varied in numbers of loci, informative sites, and amounts of missing data. This “fast-tree” approach resembles FastTree (Price et al. 2010), although it estimates two starting trees (using BIONJ [Gascuel 1997] and MP). It then optimizes the trees using rapid hill climbing including stochastic nearest neighbor interchanges (NNI), and increased tolerance on likelihood values to speed up optimization, which has the potential to reduce accuracy (for detailed steps, see Supplementary Information).

Following the inference of trees from concatenated data sets, we performed an initial quality check of the inferred phylogenies by visual assessment of the relationships, and we pruned *Muscipipra vetula* and *Spheniscus mendiculus* from trees using the `drop.tip` function in *ape* v5.7-1 (Paradis and Schliep 2019) because these appeared in positions that were unlikely.

Coalescent species tree estimation.— For the full data set and each of the six filtered data sets, we estimated individual gene trees using IQ-TREE v2.1.3 (Minh et al. 2020) under the GTR+G model, and we combined the ML trees to generate a species tree using ASTRAL v5.7.8 (Zhang et al. 2018) (Table 1, strategy 2).

Building supertrees using existing phylogenomic trees.— Supertree methods (Table 1, strategy 3) infer phylogenies from existing trees, and we identified 53 trees from 46 phylogenomic studies (McCormack, Harvey, et al. 2013;

Jarvis et al. 2014; Lamichhane et al. 2015; Nater et al. 2015; Prum et al. 2015; Bryson et al. 2016; Hosner et al. 2016; Manthey et al. 2016; Ottenburghs et al. 2016; Zarza et al. 2016; Burga et al. 2017; Reddy et al. 2017; Wang et al. 2017; White et al. 2017; Yonezawa et al. 2017; Andersen et al. 2018; Bruxaux et al. 2018; Campillo et al. 2018; Chen et al. 2018; Ferreira et al. 2018; Musher and Cracraft 2018; Younger et al. 2018; Andermann et al. 2019; Andersen et al. 2019; Everson et al. 2019; McCullough, Joseph, et al. 2019; McCullough, Moyle, et al. 2019; Oliveros et al. 2019; Sackton et al. 2019; White and Braun 2019; Harvey et al. 2020; Imfeld et al. 2020; Oliveros et al. 2020; Salter et al. 2020; Smith et al. 2020; Vianna et al. 2020; Catanach et al. 2021; Kirchman et al. 2021; Oliveros et al. 2021; McCullough et al. 2022; Vinay et al. 2022; Wang et al. 2022; Smith et al. 2023; Zhao et al. 2023; Braun et al. 2024; for details, see Supplementary Table S4), which have overlapping taxa with those included in the supermatrix data sets. After obtaining tree files representing all studies (see Supplementary Information), we reconciled the taxon names to match those in IOC v13.1 and pruned duplicate tips that represented the same species within a tree using the `drop.tip` function in *ape*.

Because the phylogenomic trees we downloaded included few taxa that overlapped among studies, we integrated them using three types of backbone trees: one from Burleigh et al. (2015) that we refer to as the “Burleigh backbone,” a second from Jetz et al. (2012) that we refer to as the “Jetz backbone,” and a “taxonomic” backbone (family-level or genus-level). See Supplementary Information for how we generated the Burleigh and Jetz backbones. We created the family-level taxonomic backbone based on taxon names in IOC v13.1 to: group individual taxa by family, cluster taxa from same family into a polytomy, cluster families from the same order into a polytomy, and cluster orders into infraclasses Palaeognathae, Galloanserae, and Neoaves. Finally, we enforced a tree topology to reflect a well-established topology: (outgroup,(Palaeognathae,(Galloanserae, Neoaves))). We constructed the genus-level taxonomic backbone similarly by clustering taxa from the same genus into a polytomy, then clustering by family, order, and infraclass and enforcing the same topology among infraclasses.

We used matrix representation with parsimony (MRP) (Baum 1992; Ragan 1992) to generate supertrees following the pipeline described in Kimball et al. (2019). Because the supertree method can suffer from source tree incongruence (Bininda-Emonds et al. 2002), we employed a user-guided weighting scheme to address topological conflicts among source trees. Specifically, we assigned different weights to input trees based on the amount of data used to infer them (Supplementary Table S4) by including from one (low weight) to eight (high weight) copies in the supertree matrix. For example, trees based on whole-genome sequencing data, such as the Jarvis TENT tree (Jarvis et al. 2014), were given a weight of eight and included in the supertree

TABLE 1. Summary of data sets, analyses, and phylogenetic trees in our initial exploration

Method	Analysis	Input data set	Tree
Supermatrix (baseline)	RAxML-NG	Full data set	RAxML-NG full data set
Supermatrix (strategy 1)	Fasttree via IQ-TREE	Full data set	Fasttree full data set
		Filter1 (indv50_sites50_loci50)	Fasttree filter1
		Filter2 (indv0_sites50_loci70)	Fasttree filter2
		Filter3 (indv0_sites90_loci50)	Fasttree filter3
		Filter4 (indv50_sites50_loci70)	Fasttree filter4
		Filter5 (indv75_sites90_loci70)	Fasttree filter5
Coalescent species tree (strategy 2)	Gene tree estimation via IQ-TREE and gene tree summary via ASTRAL	Full data set	See the Data Availability section
		Filter1 (indv50_sites50_loci50)	
		Filter2 (indv0_sites50_loci70)	
		Filter3 (indv0_sites90_loci50)	
		Filter4 (indv50_sites50_loci70)	
		Filter5 (indv75_sites90_loci70)	
Supertree (strategy 3)	Without taxonomic backbone Family backbone	PublishedTrees+Jetz+Burleigh	S1
		PublishedTrees+Jetz+Burleigh+Familybackbone	S2
	Genus backbone	PublishedTrees+Jetz+Burleigh+Genusbackbone	S3
Divide-and-conquer (strategy 4)	Without backbone	OptimalTrees	T1
	Without backbone	BootstrapTrees	T2
	Family backbone weighted 1:4	OptimalTrees+FamilyBackbone4:1	T3
	Family backbone weighted 1:2	OptimalTrees+FamilyBackbone2:1	T4
	Genus backbone weighted 1:4	OptimalTrees+GenusBackbone4:1	T5
	Genus backbone weighted 1:2	OptimalTrees+GenusBackbone2:1	T6

Note: The six filtered data sets were numbered based on total number of sites; filter1 included the highest number of sites and filter6 included the lowest number of sites.

matrix eight times. We typically weighted UCE trees as four. However, if a study included two UCE trees estimated by different approaches (e.g., methods of tree estimation or filtering strategies) but using completely or largely overlapping data, we assigned each tree a weight of two. We assigned two additional trees (Reddy et al. 2017; Yonezawa et al. 2017) a weight of two because they were based on a large number of “legacy markers” (Kimball et al. 2009) extracted from genome assemblies. Finally, we assigned a weight of one to all backbone trees.

After determining the weighting scheme, we created three supertree matrices: (1) weighted trees with the Burleigh and Jetz backbones; (2) weighted trees with Burleigh, Jetz, and family-level taxonomic backbones;

and (3) weighted trees with Burleigh, Jetz, and genus-level taxonomic backbones. Then we used CLANN (Creevey and McInerney 2005) to convert the input tree matrix to a binary (MRP) representation and generated supertrees using PAUP* v4.0 (Swofford 2003). We conducted the searches using the parsimony ratchet (Nixon 1999) as described in Kimball et al. (2019), which used code available from <https://github.com/ebraun68/ratchblock> to generate PAUP blocks that ran five tree searches with different upweighting scores. Each tree search consisted of 100 replicates and produced a strict consensus tree from these replicates after the tree search concluded. For each of the three matrices, we selected the resulting supertree as the one from the five searches that had the best parsimony score. Then we

pruned the resulting three supertrees to include only the taxa present in the full (supermatrix) data set, which resulted in 2751 taxa (seven taxa in our supermatrix were not included in published phylogenies).

Building supertrees using a divide-and-conquer approach.— Because supermatrix methods can be computationally intensive for large data sets, we also tested a divide-and-conquer approach that combined supermatrix and supertree methods by dividing the supermatrix into subsets of taxa, inferring trees from each subset using supermatrix methods, then integrating the resulting subset trees with supertree methods (Table 1, strategy 4). To begin the process, we designed three subsetting schemes that differed in the likely number of overlapping taxa shared between them: random subsets, partially stratified subsets, and fully stratified subsets.

We created 15 random subsets by randomly drawing (with replacement) 150 taxa from the total list of taxa (2760) in the full data set.

We created the partially stratified subsets by dividing all taxa in the full data set into six major groups that were recovered across many studies (Supplementary Fig. S1). Then, we randomly selected 7.5%, 3.1%, 7.8%, 6.8%, 7.4%, and 8.0% of the taxa within each group largely based on its size while avoiding oversampling suboscines, which produced a subset of 150 taxa. We repeated this selection process without replacement to create a total of 10 partially stratified subsets.

We created the fully stratified subsets by dividing all taxa in the full data set into 25 groups (Supplementary Fig. S2) that were based on taxonomy to ensure all taxa were represented at least once across the subsets and were included in trees with congeners (so sister relationships could hopefully be resolved). We set the number of taxa included in each subset under 200 to maximize computational efficiency given our resources (see Supplementary information). Because supertree analyses require overlapping taxa, we then manually selected “linker taxa” from outside each group and included them in the group membership. Preliminary analyses showed that using identical linker taxa across fully stratified subsets placed the linker taxa in unexpected positions in the resulting tree. Therefore, we used distinct linker taxa for each subset, which resolved this issue.

We created a total of 50 subsets across all schemes. We extracted subset alignments from the aligned, concatenated, full data set. Then, we used IQ-TREE v2.1.3 (Minh et al. 2020) to infer the “best” ML phylogenies and generate 1000 ultrafast bootstrap replicates for each subset using the GTR+R4 model.

We followed the same weighted-tree search approach described above to infer a set of supertrees representing all taxa from the 50 “best” ML subtrees. Specifically, we created five supertree matrices using: (1) the 50 best

ML subtrees where each tree was given a weight (w) of one ($w = 1$); (2) the 50 best ML subtrees ($w = 4$) and the family-level backbone tree ($w = 1$); (3) the 50 best ML subtrees ($w = 2$) and the family-level backbone tree ($w = 1$); (4) the 50 best ML subtrees ($w = 4$) and the genus-level backbone tree ($w = 1$); and (5) the 50 best ML subtrees ($w = 2$) and the genus-level backbone tree ($w = 1$).

We also built 1000 MRP matrices (each with 50 trees) from the bootstrap replicates by sampling and combining replicates from the subsets in the order they were generated: bootstrap replicate tree one from all 50 subsets combined to form MRP matrix one, bootstrap replicate tree two from all 50 subsets combined to form MRP matrix two, et cetera. Then we performed the tree search process described above for each MRP matrix to produce a set of 1000 phylogenomic supertrees that we summarized to a 50% majority rule consensus using SumTrees (Sukumar and Holder 2010). We pruned the six supertrees generated from the steps above to include only the taxa present in the full (supermatrix) data set.

Analyzing Tree Distances

To visually represent differences between the various trees we inferred, we rooted trees on the crocodylian outgroup and used ete3 (Huerta-Cepas et al. 2016) to calculate pairwise normalized Robinson–Foulds distances (Robinson and Foulds 1981) between the two trees inferred from the full data set, the six trees inferred from the filtered data sets, the three trees inferred from the supertree analyses, and the six trees inferred using the divide-and-conquer approach (Table 1). ASTRAL species trees were not included (see Results). We used the write.nexus.dist function in phangorn v2.11.1 (Schliep 2011) to create a NEXUS block of the pairwise Robinson–Foulds distances, and we used PAUP* v4.0 (Swofford 2003) to infer a neighbor-joining (NJ) “tree-of-trees” that we rooted at the midpoint.

Testing for Clade Monophyly

Sangster et al. (2022) and earlier work (Chen and Field 2020; de Queiroz et al. 2020; Sangster and Mayr 2021) highlighted several clades near the base of the avian tree that are very likely to reflect the true species tree. Modern taxonomies, such as IOC, eBird/Clements (Clements et al. 2023), and Howard & Moore (Dickinson and Christidis 2014), now circumscribe orders, families, and genera in ways that largely align with recent phylogenetic insights. However, no current taxonomy is without limitations. Some families and genera continue to be refined as more information becomes available. Although there are almost certainly some named taxa that do not represent clades in the true species tree, the majority of named groups are likely to be expected clades. We compared how reliably the dif-

ferent tree inference methods resolved these expected clades across the avian phylogeny. These include orders, families, and genera recognized by IOC v13.1, as well as 33 high-level clades (e.g., superorder, infraclass). We generally assumed that a method was more reliable when it recovered a larger number of these groups as monophyletic (e.g., [Portik and Wiens 2021](#)). To perform these analyses, we first excluded clades that were only represented by a single species. Then we used the AssessMonophyly function in MonoPhy ([Schwery and O'Meara 2016](#)) to calculate how many of the 410 evaluated genera, 138 evaluated families, 40 evaluated orders, and 33 evaluated high-level clades were not resolved as monophyletic.

Summarizing Compute Time

We summarized and compared the compute time required for the tree inferences described above. To increase our computational capacity, analyses were run across several different computing systems: HPC@LSU (RAXML-NG analysis; <https://www.hpc.lsu.edu/>), AMNH Huxley HPC (initial fasttree analyses and ASTRAL analyses; <https://www.amnh.org/research/computational-sciences>), and UF HiPerGator (supertree and divide-and-conquer analyses; <https://www.rc.ufl.edu/about/hipergator/>). For each analysis, we tallied the CPU hours spent for tree searches (including bootstrap replicate searches if applicable) and optimization, and we collected the total cluster utilization for each SLURM job. For the RAXML-NG analysis of the full data set, we combined the CPU time for the random and the MP starting trees. For the divide-and-conquer analyses, we summed the CPU hours spent for tree search across 50 subsets. Because the supertree component for the divide-and-conquer analyses used very little CPU time compared with the subset concatenation analysis, we added it directly to the total CPU time spent (for the bootstrap trees, time for 1000 runs was added). For the regular supertree analyses, we presented the PAUP tree search time and added time for MRP matrix construction to the total CPU hours spent. To account for variations in CPU hardware performance across the three computing systems, we used the base and turbo clock speed to calculate the theoretical minimum and maximum giga floating-point operations per second (GFLOPS; 1 GFLOPS = 10^9 FLOPS) per core ([Supplementary Table S5](#)). This metric was then used to evaluate the relative performance of each computing system and to adjust the CPU cost accordingly (adjusted CPU time = CPU hours * GFLOPS).

Tests on Two Filtered Data Sets

Generating the distance matrix and BIONJ starting tree in the initial fasttree analyses was time-consuming

for our data sets. However, the likelihood of the resulting fasttree was only slightly improved compared with the MP starting tree, and the MP starting tree was always much better than the BIONJ tree ([Supplementary Table S6](#)). To improve fasttree search and optimization, we examined the role of the starting tree using two filtered data sets (filter1 and filter3). We chose these filter sets due to their contrasting patterns of expected clade recovery in initial exploration: filter1 performed well deeper in the tree but poorly at the tips, whereas filter3 showed the opposite pattern. Fasttree searches normally use two starting trees (MP and BIONJ); however, users can supply their own starting tree to bypass the default starting tree estimation process. We performed a total of 24 additional tree searches for each data set with different starting trees (see [Supplementary Information](#)). We evaluated the log likelihoods of the starting tree and optimal tree and assessed expected clade recovery for the final ML tree in each analysis ([Supplementary Table S7](#)).

Based on the tests using filter1 and filter3, we found that searches initiated with BIONJ and MP starting trees required a large amount of time, had a much lower likelihood, and resulted in worse expected clade recovery than the initial exploration ([Supplementary Fig. S3](#) and [Supplementary Table S7](#)). In contrast, fasttrees built using only MP starting trees derived from the same filtered data set used for the ML search consistently had much better likelihoods than those derived from other filtered data sets. These results suggest a straightforward method to improve the speed and reproducibility of fasttree searches: avoid generating the BIONJ tree and instead conduct multiple searches using MP starting trees generated from the same data set used for the fasttree search.

New Fasttree Method with MP Starting Trees

We used Parsimonator v1.0.2 (<https://github.com/stamatak/Parsimonator-1.0.2>) to estimate four MP starting trees (parsA, parsB, parsC, and parsD; different random number seeds for each search) for each of the full and 27 filtered data sets. Each MP starting tree was used to run a fasttree analysis in IQ-TREE v2.2.2 ([Nguyen et al. 2015](#)) with parsA and parsB using the GTR+G model and parsC and parsD using the FreeRates model (GTR+R4). Two filtered data sets were identical to each other (indv75_sites50_loci90 and indv75_sites70_loci90); therefore, we performed only one set of analyses for these two data sets. This resulted in a total of 108 new fasttrees, four for each data set ([Table 2](#)). We evaluated their performance in expected clade recovery and summarized the total CPU time spent. We z-transformed each locus-based summary statistic across all filtered data sets and plotted using ComplexHeatmap with hierarchical clustering ([Supplementary Fig. S4](#)). From each cluster, we selected a representative data set

TABLE 2. Summary of data sets, analyses, and phylogenetic trees using modified methods

Method	Analysis	Input data set	Tree
Fasttrees with MP starting trees	Fasttree via IQ-TREE using parsimony starting trees estimated by Parsimonator	Full data set: GTR+G (Replicates A,B), GTR+R4 (Replicates C,D) 27 filtered data sets: GTR+G (Replicates A,B), GTR+R4 (Replicates C,D)	New fasttrees, four for each data set (GAMMA parsA, GAMMA parsB, FreeRates parsC, FreeRates parsD)
Hybrid supertree	Include a fasttree backbone	PublishedTrees + Fasttree Fulldata PublishedTrees + Fasttree filter1-6 PublishedTrees + Fulldata_FreeRates_parsD PublishedTrees + indv0_sites50_loci50_GAMMA_parsB	supertrees with different fasttree as backbone, without taxonomic backbone
	Include a fasttree and a family backbone	PublishedTrees + Fasttree Fulldata + Familybackbone PublishedTrees + Fasttree filter1-6 + Familybackbone PublishedTrees + Fulldata_FreeRates_parsD + Familybackbone PublishedTrees + indv0_sites50_loci50_GAMMA_parsB + Familybackbone	Nine hybrid supertrees with different fasttree plus a family-level taxonomic tree as backbones
Hybrid divide-and-conquer	Include a fasttree as backbone	OptimalTrees + Fasttree Fulldata OptimalTrees + Fasttree filter1-6 OptimalTrees + Fulldata_FreeRates_parsD OptimalTrees + indv0_sites50_loci50_GAMMA_parsB	Nine hybrid divide-and-conquer trees with different fasttree as backbone, without taxonomic backbone
	Include a fasttree and a genus backbone	OptimalTrees + Fasttree Fulldata + GenusBackbone OptimalTrees + Fasttree filter1-6 + GenusBackbone OptimalTrees + Fulldata_FreeRates_parsD + GenusBackbone OptimalTrees + indv0_sites50_loci50_GAMMA_parsB + GenusBackbone	Nine hybrid divide-and-conquer trees with different fasttree plus a genus-level taxonomic tree as backbones

that performed best in recovering expected clades. We only present the best fasttree for these representative data sets in the main text (see complete results in [Supplementary Table S8](#)).

Hybrid Approaches

We tested whether fasttrees could improve the supertree and divide-and-conquer methods when used as backbone trees. Unlike the Jetz+Burleigh backbones used initially, our fasttrees included all taxa in the analyses, potentially providing a better backbone to compensate for limited overlap among source trees. Additionally, because our fasttrees were estimated from phylogenomic data, they may offer a more accurate representation of relationships, potentially reducing the need for taxonomic backbones. We referred to these new approaches as the “hybrid supertree approach” and “hybrid divide-and-conquer approach” ([Table 2](#)).

We used the two best new fasttrees (based on expected clade recovery) and seven initial fasttrees as the backbone tree in supertree and divide-and-conquer

analyses ([Table 2](#)). For the hybrid supertree approach, we conducted two sets of nine analyses (with or without a family-level taxonomic backbone), each analysis with a different fasttree as the backbone. Each backbone was given a weight of one, and source trees were given different weights based on the amount of data used to infer them, as described above. For the hybrid divide-and-conquer approach, we also ran two sets of analyses, each with nine trees estimated: (1) using only a fasttree as the backbone with the 50 best ML subtrees and the fasttree backbone each given a weight of one; and (2) using a fasttree backbone and a genus-level backbone with the 50 best ML subtrees given a weight of two and the backbones given a weight of one. We then followed the same steps described above to build a binary MRP tree matrix in CLANN and generate supertrees using PAUP*. Similarly, we evaluated the performance in expected clade recovery for final output trees ([Supplementary Table S9](#)). When summarizing the total CPU time spent, we added in the compute time for generating each MP starting tree and the fasttree. All new fasttrees, MP starting trees, and hybrid approaches were run on UF HiPerGator HPC.

Molecular Dating

We applied a total of 43 fossil calibrations for node-dating analyses ([Supplementary Table S10](#)) following best practices proposed by [Parham et al. \(2012\)](#), and we assigned minimum and maximum possible ages to each calibrated node in our phylogeny. Additional information regarding the fossils selected to calibrate divergence time analyses is presented in the [Supplementary Information](#).

Then, due to the size of the resulting trees, we used TreePL ([Smith and O'Meara 2012](#)) to estimate divergence times for the (1) RAxML-NG tree inferred from the concatenated, full data set; (2) two fasttrees using new fasttree methods based on the full data set and the filtered data set `indiv0_sites50_loci50`; (3) two supertrees (one from initial exploration and one from the hybrid approach); and (4) two divide-and-conquer trees (one from initial exploration and one from the hybrid approach). For the four supertrees and divide-and-conquer trees, we used IQ-TREE2 v.2.2.2 ([Nguyen et al. 2015](#)) to optimize the tree branch lengths (–treefix) under both GTR+G and GTR+R4 models using the filtered data set with the smallest amount of missing data (`indiv0_sites90_loci90`). TreePL allows for varying rates across branches but penalizes rate differences over the tree with a rate smoothing parameter, so we identified the optimal rate smoothing parameter through cross-validation that tested 10 values (start = 1e-07; stop = 10,000). We also used the “prime” option to identify the best optimization parameters and the “thorough” option to allow the program to iterate until convergence.

We extracted crown ages only for groups that were monophyletic across seven time trees and compared the age of each group across trees. We also compared the time estimates for 12 major groups (that have been consistently resolved across studies and that represent both ancient and recently diverged clades as well as both fast- and slow-evolving clades) to those in other studies ([Claramunt and Cracraft 2015](#); [Prum et al. 2015](#); [Kimball et al. 2019](#); [Kuhl et al. 2021](#); [Brocklehurst and Field 2024](#); [Claramunt et al. 2024](#); [Stiller et al. 2024](#); [Wu et al. 2024a](#)). Divergences estimated under GTR+G and GTR+R4 models were very similar (see Data Availability); thus, only results from the GTR+R4 model were used for presentation. We also computed relative divergence time for these clades by scaling the divergences to Neognathae.

RESULTS

Taxon Sampling

Our UCE data matrix contained DNA sequence alignments for 5121 target captured loci, with an average length of 665 base pairs (bp) and a total of 2,047,980 parsimony informative sites. The full data set contained 2758 tips (including two crocodylian outgroups); mem-

bers of all 44 extant bird orders and one extinct order (Dinornithiformes); 250 of 253 (98.8%) extant bird families and one extinct family (Emeidae); 1081 genera; and 2747 unique species.

Data Set Characteristics and Filtering

Data heterogeneity was evident in descriptive statistics for individual taxa. For instance, taxa showed considerable variation in locus count, sequence length, and individual-based parsimony informative sites both within and between studies ([Supplementary Fig. S5](#)). PCA of these summary statistics revealed distinct clusters corresponding to their source data sets ([Supplementary Fig. S6](#)). As anticipated, more stringent filtering schemes substantially increased homogeneity among studies and reduced the amount of missing data. However, these improvements reduced the number of informative sites ([Supplementary Fig. S5](#)).

Baseline Phylogeny

The RAxML-NG tree of the full concatenated data set recovered all 33 high-level clades identified by [Sangster et al. \(2022\)](#), all 40 evaluated orders (excluding monotypic or single-sampled orders), all but two of the 138 evaluated families, and all but 38 of the 410 evaluated genera ([Fig. 2](#); [Supplementary Fig. S7](#)).

Although the RAxML-NG tree appeared to provide an accurate estimate of avian phylogeny based on expected clade recovery, generating this tree required significant computational resources—approximately 428,000 CPU hours for the primary search and additional 323,000 CPU hours for a limited number of bootstrap analyses.

Initial Exploration

We explored four alternative approaches ([Table 1](#)) that were more computationally efficient than standard ML: (1) implementing a fast ML estimation approach, (2) estimating individual gene trees and combining them into a species tree, (3) combining source trees into a supertree, and (4) using a divide-and-conquer strategy in which trees were estimated from data subsets and then combined into a supertree. The primary goal of these analyses was to determine whether any of these computationally efficient methods could produce trees as accurate as the RAxML-NG tree.

The fasttree ([Table 1](#), strategy 1) estimated from the full data set did not perform as well as either the RAxML-NG tree or the best trees from other approaches ([Fig. 3](#)). Filtering appeared to improve the performance of fasttree analyses, with the best results based on the expected clade recovery criterion observed in trees inferred from the least aggressively filtered data sets (filter1 and filter2). By contrast, the most aggressively fil-

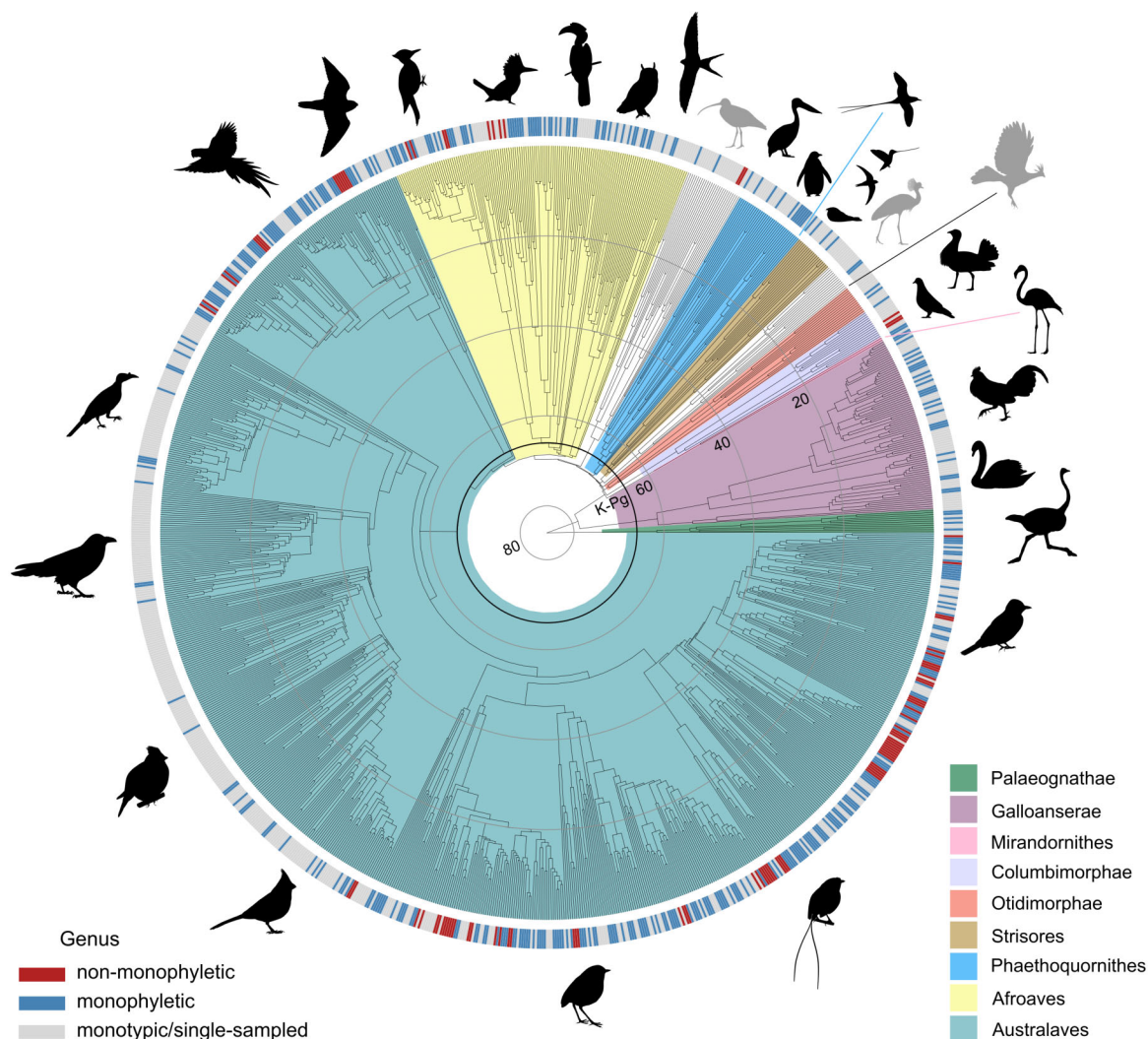


FIGURE 2. A genus-level RAxML-NG tree with branch lengths converted to divergence time using TreePL. Major bird clades are color-coded, while three lineages (Gruiformes, Charadriiformes, and Opisthocomiformes; see Reddy et al. 2017) that were not placed within a strongly corroborated superordinal clade remain uncolored (silhouettes in gray). Colored bars in the outer ring indicate genera that are monophyletic (blue; $n = 372$) and non-monophyletic (red; $n = 38$) in this phylogeny. Monotypic genera ($n = 334$ with a single species currently recognized in IOC World Bird List v13.1) and genera represented by a single sample in our data set ($n = 337$) are gray. The concentric gray circles and adjacent integer values indicate 20 Ma time intervals. The black circle indicates the K-Pg boundary at 66 Ma. See Supplementary Figure S7 for a version of this tree with tip labels.

tered data sets (filter5 and filter6) performed poorly with clade recovery similar to that of the full data set fasttree, suggesting diminishing returns with overly stringent filtering.

The ASTRAL species trees (Table 1, strategy 2) recovered substantially fewer expected clades than either the RAxML-NG tree or the fasttrees, regardless of the filtering procedure (or lack thereof) used to generate the alignments for gene tree estimation. The total number of unresolved groups ranged from 144 to 207 and adjusted CPU time (CPU hours * GFLOPS) ranged from 21,341 to 1,977,494 (Supplementary Table S11).

For the supertree analysis (Table 1, strategy 3), the supertree constructed without taxonomic backbones (S1) performed poorly in recovering expected clades (Fig. 3). In contrast, the two supertrees with taxonomic backbones (S2 and S3) performed as well as, or slightly better than, the RAxML-NG tree in terms of expected clade recovery while still requiring minimal compute time (Fig. 3).

The divide-and-conquer approach (Table 1, strategy 4) without taxonomic backbones outperformed the supertree without backbones in recovering expected clades (Fig. 3). However, performance comparable to the RAxML-NG tree was achieved only when a genus back-

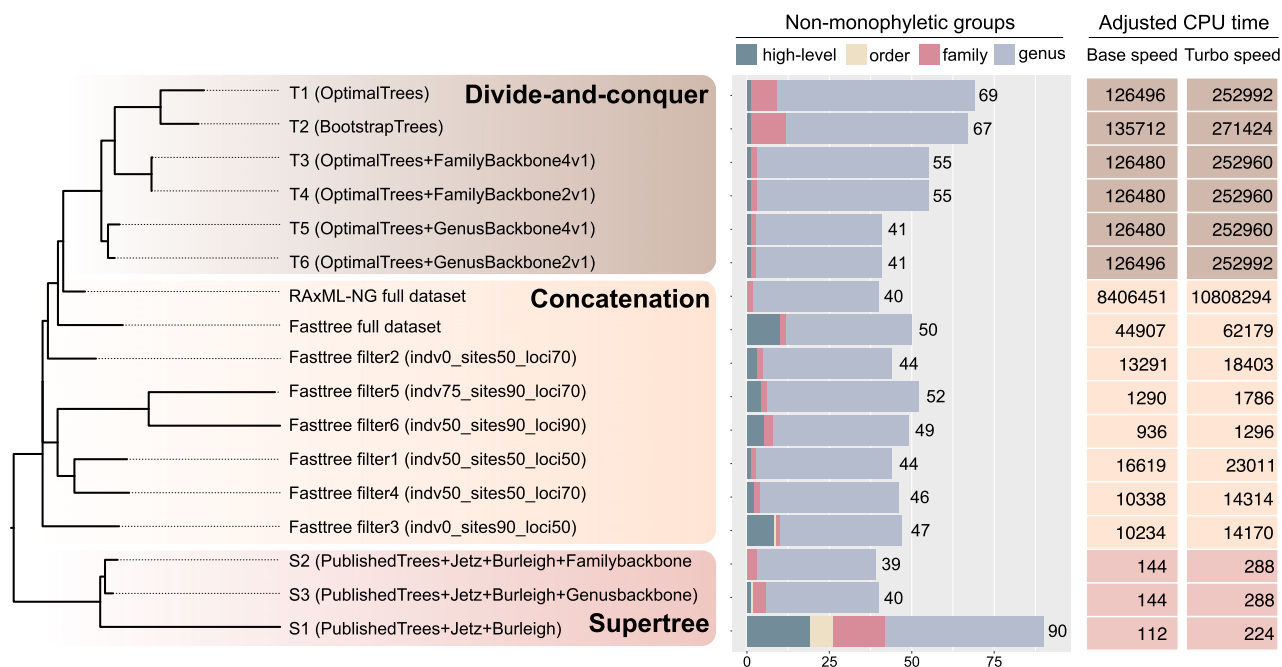


FIGURE 3. Similarity and performance of trees from the initial exploration. The phylogram represents tree similarity measured with normalized Robinson–Foulds distances and was constructed using neighbor-joining followed by midpoint rooting. ASTRAL results are not included but can be found in [Supplementary Table S11](#). For each tree, we summarized the number of high-level clades, orders, families, and genera recognized by IOC World Bird List v13.1 that are not monophyletic in the tree; therefore, the higher the number, the more non-monophyletic groups. Non-monophyly may be due to artifacts in phylogenetic inference or taxonomic classification that requires revision. The adjusted CPU time (CPU hours * GFLOPS) required for each analysis is shown at the right (see Materials and Methods for details).

bone was included. Despite requiring the estimation of input trees from the supermatrix, this method was much more computationally efficient than the RAxML-NG analysis (Fig. 3).

The two divide-and-conquer trees using the genus backbone (T5 and T6) performed well overall but exhibited polytomies within heavily sampled passerine families, such as Tyrannidae and Thamnophilidae, as well as among some oscine families. Notably, these polytomies were not observed in [Oliveros et al. \(2019\)](#) and [Harvey et al. \(2020\)](#), which were the sources of most of the passerine data. The number of polytomies decreased when the weight of the source trees relative to the genus backbone was reduced (lower in T6 [2:1] vs. higher in T5 [4:1]; see [Supplementary Information](#) for details on comparing polytomies). However, this adjustment did not affect the recovery of expected clades.

The tree-of-trees (Fig. 3) indicated that the method of inference (supermatrix, supertree, or divide-and-conquer) strongly influenced topological similarity. Notably, supertree and divide-and-conquer methods formed distinct clusters. For the supertrees, this clustering may reflect biases introduced by relationships within the source trees, which differed from those inferred using other methods. Similarly, the clustering of divide-and-conquer analyses likely stems from the use of the same underlying subset trees (or their

bootstrap consensus), which may have contributed unique relationships within the data subsets. By contrast, the fasttrees did not form a single cluster, and branch lengths in the NJ tree indicated greater variation among these analyses compared to the other methods. This increased variation is expected, given that the fasttree data sets differed in content due to filtering.

Fasttrees with MP Starting trees

We conducted four searches on the full data set and each of the 27 filtered data sets. Analysis of expected clade recovery for all new fasttrees ([Supplementary Table S8](#)) revealed that one fasttree from the full data set (using an MP starting tree with the GTR+R4 model in replicate search D, i.e., FreeRates parsD) matched the RAxML-NG tree in both the number and identity of expected clades (Figs. 4 and 5). This best full data set fasttree closely approximated the RAxML-NG tree in tree space (Fig. 4), but it was far more computationally efficient (69- to 178-fold difference in the adjusted CPU costs between the two analyses, depending on the dynamic CPU speed).

We compared the performance of filtered data sets to evaluate the effects of different filtering strategies. At the genus level, data sets filtered with indv0 and loci50 (keeping all taxa within specific loci and retain-

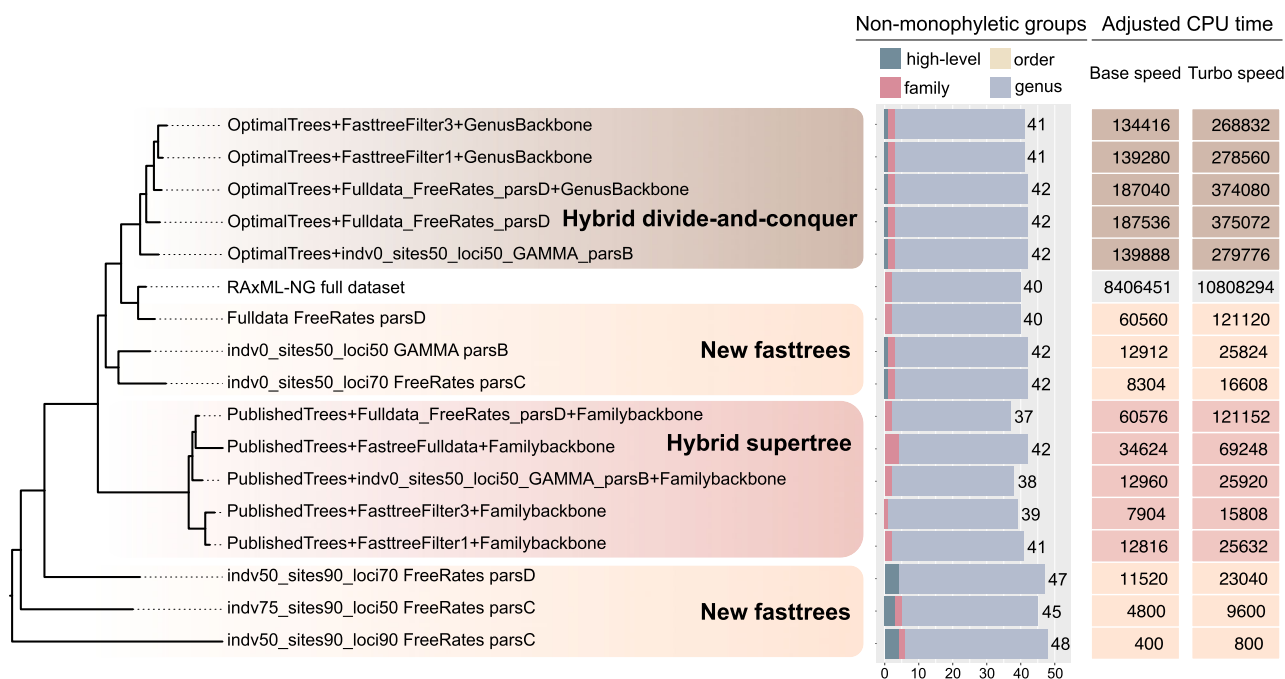


FIGURE 4. Similarity and performance of trees from the modified methods. Here, we only present the representative trees for each approach. Full results can be found in [Supplementary Tables S8 and S9](#). For the two hybrid approaches, we added in the time for running the backbone tree. For the new fasttrees with MP starting trees, we summarized the compute time for running four fasttrees analyses for each data set (using different MP starting trees under GTR+G [parsA and parsB] or GTR+R4 [parsC and parsD] model) and present the total time of four runs.

ing loci sampled in $\geq 50\%$ of taxa) achieved the best expected clade recovery. For high-level clades, data sets filtered with sites50 (removing alignment columns where $\geq 50\%$ of taxa were gaps or missing) performed best. In contrast, more aggressive filtering approaches, such as loci90 (retaining loci sampled in $\geq 90\%$ of taxa) and indv75 (keeping taxa with $\geq 75\%$ of sequence completeness), consistently resulted in poorer clade recovery. As expected, filtering reduced the number of sites and CPU time was positively correlated with the size of the supermatrix across all fasttree analyses ($R^2 = 0.8$; [Supplementary Fig. S8](#)). Although we observed no consistent pattern in clade recovery between trees estimated with FreeRates and GAMMA models, GAMMA models generally required less compute time.

Hybrid Supertrees and Hybrid Divide-and-Conquer Trees

Using a fasttree backbone in the hybrid supertree approach led to poor clade recovery, with some iterations performing worse than our initial analyses using the Jetz+Burleigh backbones ([Fig. 4](#) and [Supplementary Table S9](#)). However, as in the initial analyses, adding a taxonomic backbone greatly improved performance, with several hybrid supertree analyses recovering more expected clades than the RAxML-NG tree. Despite these improvements, a better backbone did not eliminate the novel relationships introduced in the supertree analyses.

Hybrid supertrees still produced topologies that were the most divergent from those inferred by RAxML-NG, our best new fasttrees, or our best hybrid divide-and-conquer trees ([Fig. 4](#)).

The hybrid divide-and-conquer trees were similar to the RAxML-NG tree ([Fig. 4](#)). However, even when using a fasttree with strong expected taxa recovery (e.g., the fasttree fulldata parsD), these trees recovered fewer expected clades than the RAxML-NG analysis. Although the inclusion of a taxonomic backbone provided some improvement, none of the hybrid divide-and-conquer trees outperformed the best hybrid supertrees ([Fig. 4](#)). Additionally, some polytomies observed in the initial analyses persisted, even with the inclusion of both the fasttree and a taxonomic backbone.

Divergence Time Estimation

Divergence time estimates for key nodes were generally similar across our seven trees ([Fig. 7](#)), despite being estimated using different methods and data sets. Lower-level ranks (e.g., genus) in general showed higher variation in crown ages across trees when compared with higher-level ranks ([Fig. 7a](#)). However, the number of outliers (points that fell outside 1.5x the interquartile range for all clades of the same rank) was smaller as a proportion of the total clades considered in lower-level ranks. Recent studies also show

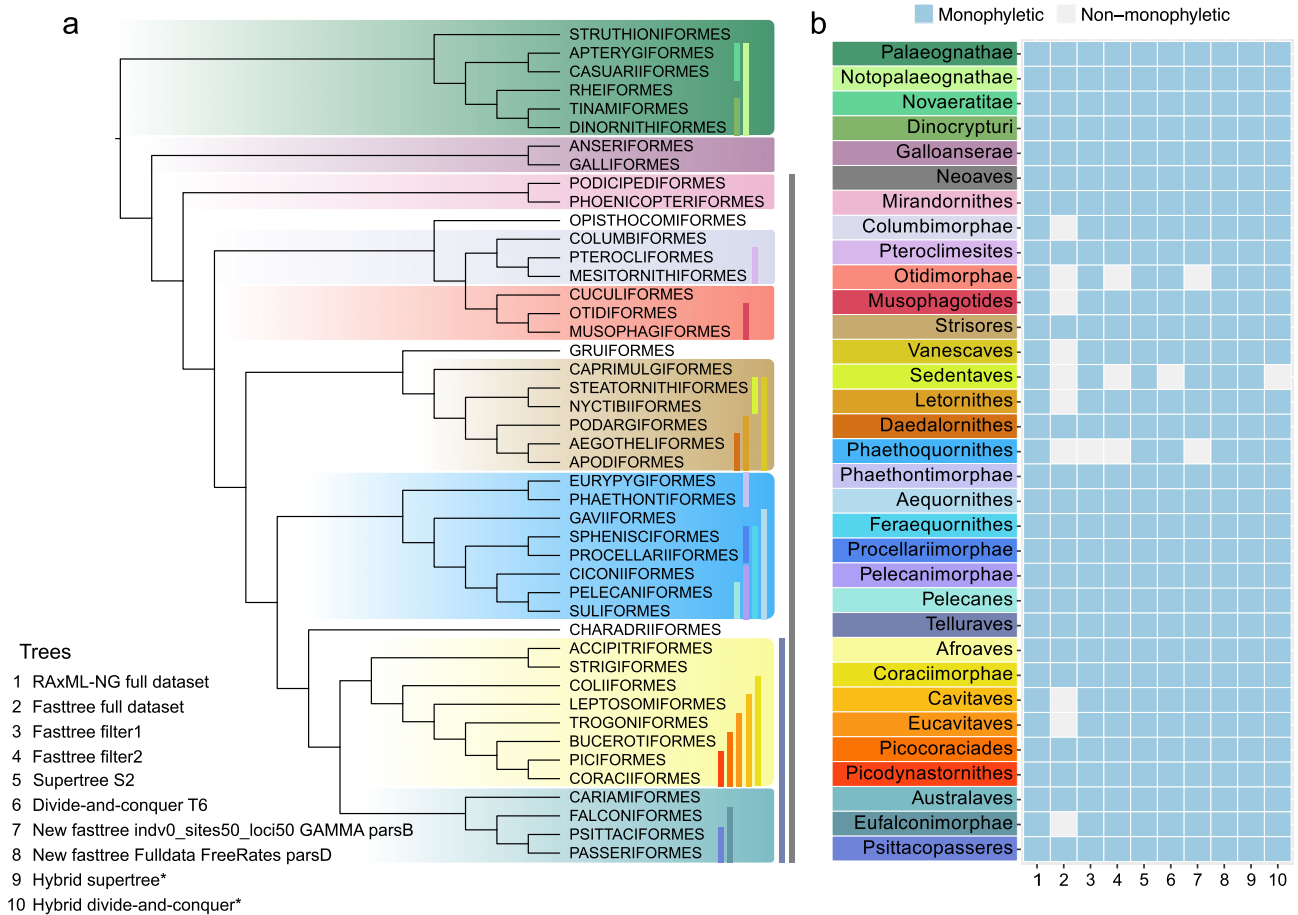


FIGURE 5. (a) Cladogram showing relationships among orders in the best fasttree using the full data set and the new fasttree approach with MP starting trees (tree no. 8). Vertical bars next to order names indicate composition of high-level clades. (b) We compared recovery of high-level clades in trees estimated from the full data set (both by RAXML-NG and initial fasttree analysis via IQ-TREE) and trees with the best expected clade recovery using various approaches: two initial fasttrees using filtered data sets, the initial supertree and divide-and-conquer trees, the new fasttrees using MP starting trees (filtered data set and full data set), and the trees using hybrid supertree and divide-and-conquer methods.

broadly similar relative divergence times (to Neognathae) for comparable groups (Fig. 7b), although there were differences among time trees (especially for published studies) in the absolute divergence times (Fig. 7c).

DISCUSSION

Baseline Phylogeny and Expected Clade Recovery

The RAXML-NG tree provided a reliable estimate of the bird phylogeny, and most cases of non-monophyly at lower taxonomic levels matched results from recently published phylogenomic studies (e.g., Harvey et al. 2020; Smith et al. 2023). Some instances of non-monophyly likely reflected artifacts, such as limited taxon sampling or insufficient sequence data, particularly from historical museum specimens, whereas others appear to reflect the true phylogenetic relationships of genera or families for which formal taxonomic revision

is pending (e.g., *Tyrannetes* nested in *Neopelma* [Leite et al. 2021], *Antilophia* in *Chiroxiphia* [Zhao et al. 2023], and Tityridae divided into Tityridae *sensu stricto*, Onychorhynchidae, and Oxyruncidae [Oliveros et al. 2019]). However, the RAXML-NG analysis required substantial computational resources, which was expected given the long-recognized challenges of large tree searches under the likelihood criterion (reviewed by Yang and Rannala 2012). The recently introduced Early Stopping version of RAXML-NG, which offers up to a 5-fold speedup for large DNA data sets and up to 10-fold speedup when using MP starting trees (Togkousidis et al. 2025), may reduce some of these computational demands. Conversely, incorporating MP starting trees to fasttree approaches significantly reduces the computational burden while producing trees that appear to be of approximately equal quality—providing a promising alternative for scaling future phylogenetic inferences including thousands of loci to even larger numbers of tips (5000+).

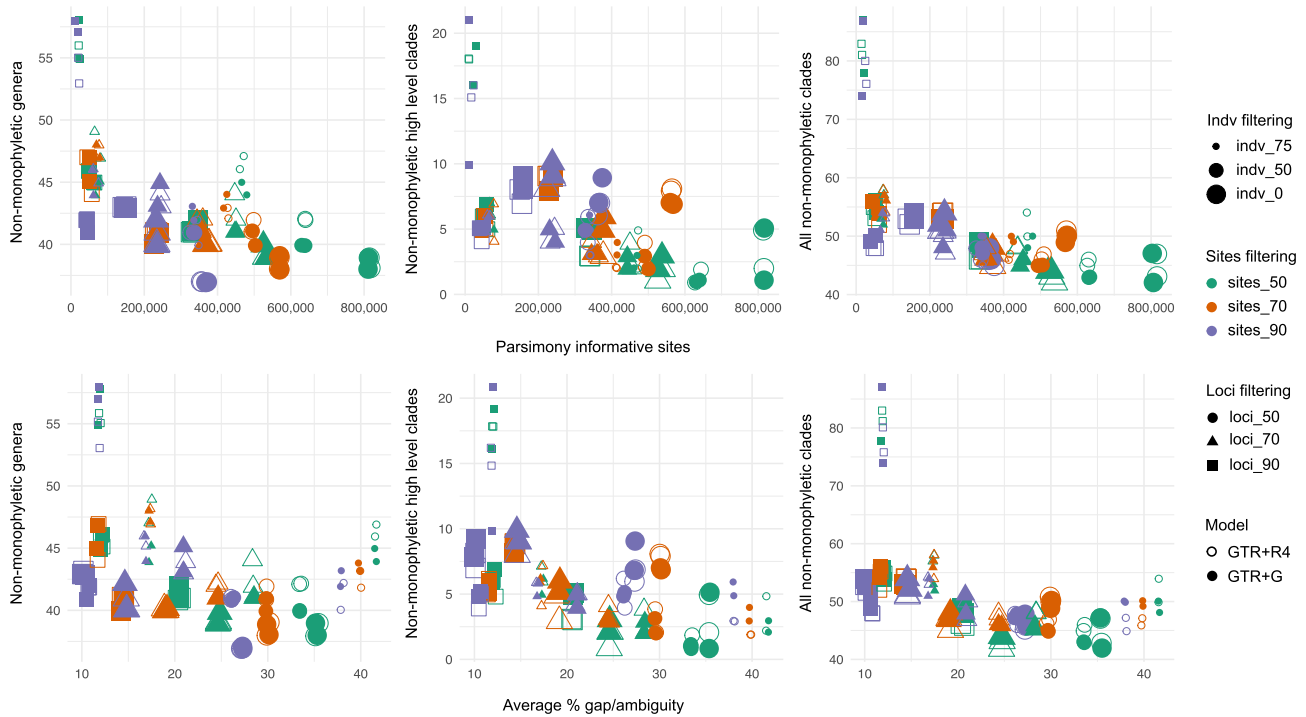


FIGURE 6. A comparison between the number of unresolved expected clades (genera, high-level clades, and all expected clades combined) and parsimony informative sites (top panels), as well as average proportion of gaps and ambiguities (“-”, “?” or “N”) across all locus alignments for the data set (bottom panels). For each filtered data set, four fasttrees with different parsimony starting trees were evaluated. We applied jitter to points when two shapes were completely overlapping so that both shapes would be visible.

Fasttree Approaches

As noted above, we evaluated alternative analytical approaches that might offer similar or even greater accuracy while requiring fewer computational resources than RAxML-NG. Our initial exploration of computationally efficient methods found that fasttrees, while not as accurate as the RAxML-NG tree or the best-performing supertrees and divide-and-conquer trees, still demonstrated relatively good recovery of expected clades (Fig. 3). Previous studies found that trimming the alignments did not improve expected clade recovery (Tan et al. 2015; Portik and Wiens 2021). However, this was not the case for our initial fasttree analyses, because the fasttree based on the full data set exhibited poorer clade recovery than most of the filtered data sets. This result suggests that the heterogeneity of the full data set may interfere with fasttree searches, unlike the RAxML-NG analysis, which appeared more robust to heterogeneity.

We improved the fasttree search and optimization process by conducting four replicate searches, each initiated using an MP starting tree. This modification resulted in a best full data set fasttree that achieved phylogenetic accuracy comparable to the RAxML-NG tree, yet with a substantially reduced computational burden (Fig. 4). Although the two trees differed in the arrangement of Otidimorphae, Columbimorphae, and Opistho-

comiformes (Supplementary Fig. S9), the relationships among high-level clades at the base of Neoaves remain a particularly challenging phylogenetic problem (reviewed by Braun et al. 2019), with no consensus achieved to date (cf. Stiller et al. 2024; Wu et al. 2024a).

In contrast to our attempts to improve search efficiency, data set filtering approaches yielded mixed results. Unlike our initial analyses, filtering to remove missing data did not enhance new fasttree performance in recovering expected clades, likely because filtered data sets also had fewer parsimony informative sites (Fig. 6). This result agrees with the findings in Tan et al. (2015) and Portik and Wiens (2021) that filtering did not increase expected clades recovery. Additionally, we found that site filtering had a greater impact on high-level clade recovery, whereas locus and individual filtering more strongly influenced resolution of expected genera. The most effective filtering strategy likely depends on the taxonomic level of interest, and a significant benefit of the new fasttree approach is that testing various filtering strategies and models is more feasible due to the significantly reduced compute time. This efficiency also makes it possible to incorporate multiple replicates of tree search to account for stochasticity. As phylogenomic data sets continue to grow in size, further advancements in computational efficiency for tree estimation will remain essential.

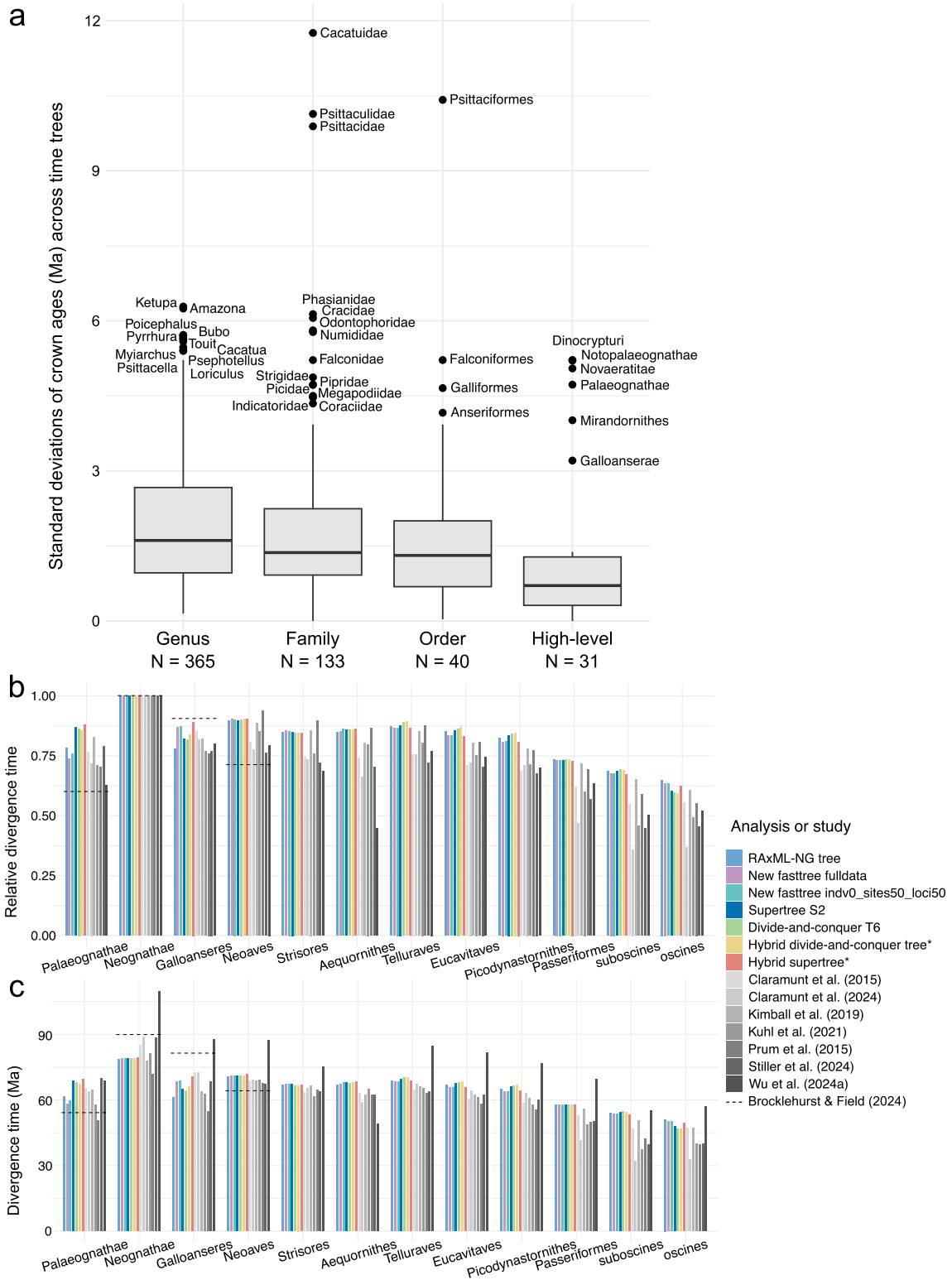


FIGURE 7. Variation in estimated divergence times for different analyses. (a) Standard deviations of crown ages (Ma) for evaluated clades in four ranks (genus, family, order, and high-level clades) were calculated using our time trees. Only monophyletic groups were evaluated. The plot of standard deviations shows their median, interquartile range (box), and 1.5x the interquartile range (whiskers). (b) Crown ages for 12 major avian clades with relative divergence time (to Neognathae) for our time trees. Crown ages from eight published time trees are included for comparison. (c) Crown ages for 12 major avian clades shown as absolute divergence time.

Species Tree Methods on Heterogeneous Data Sets

Results from the ASTRAL analyses are consistent with previous studies, which have shown that poor sequence recovery and missing data can bias gene tree summary methods (Liu et al. 2010; Springer and Gatesy 2014; Hosner et al. 2016; Xi et al. 2016; Zhao et al. 2025). One contributing factor is the distribution of informative sites in UCE alignments, which are disproportionately located near the ends of the alignments (Faircloth et al. 2012). These regions may be underrepresented when sequence recovery is poor, particularly in lower-quality samples such as those derived from historical museum specimens. Consequently, taxa with poor sequence recovery may be misplaced in estimated gene trees or excluded from certain gene trees altogether, leading to inaccuracies in the ASTRAL tree. Improving ASTRAL trees would entail excluding lower-quality samples and result in a tree with many fewer tips. Overall, ASTRAL was not an accurate method for estimating macrophylogeny with this type of heterogeneous UCE data, even when using the more homogenous filtered subsets. Additionally, ASTRAL was less computationally efficient than many of the other methods tested (Supplementary Table S11).

Supertree and Divide-and-Conquer Approaches

Despite being computationally efficient, the supertrees contained novel nodes that contradicted all input trees, potentially due to issues of hidden support (e.g., Gatesy et al. 2004; Wilkinson et al. 2005). Although signals from the input phylogenomic trees should dominate the supertree topology due to their higher weights relative to the backbones, novel relationships likely arose from topological incompatibilities or asymmetric taxon sampling in the published phylogenomic trees used as input. These issues appeared to be intrinsic to the structures of the input trees (see examples in Supplementary Information). Consequently, hybrid supertrees still produced topologies that were the most divergent from other trees (Fig. 4). This outcome may be explained by the reliance of supertree methods on input trees generated using different analytical approaches by different investigators, as we combined trees from 46 distinct phylogenomic studies. Although the compute time required for supertree analyses was minimal (Fig. 3), this does not include the time needed to locate and code the source trees for analysis.

Overall, we were able to produce supertrees that provided reasonably accurate representations of the Avian Tree of Life, but the methods were not straightforward. Consistent with previous studies, we found that incorporating backbones was critical for improving taxonomic overlap (Redelings and Holder 2017; Kimball et al. 2019; McTavish et al. 2024). An alternative or complementary approach involves pruning problematic

taxa from the source trees (Bininda-Emonds et al. 2002) or upweighting more accurate source trees (Bininda-Emonds and Sanderson 2001). Although these strategies can improve phylogenetic accuracy, they require prior knowledge and subjective decisions about phylogenetic relationships, which may not always be feasible or unbiased.

Compared with typical supertree approaches, the divide-and-conquer method has advantages, as the individual trees integrated using supertree techniques are generated under consistent programs, parameter settings, and computing platforms. This approach establishes a direct link between sequence data and supertree estimation, addressing the data-dissociation problem inherent in traditional supertree methods (e.g., Moore et al. 2006). However, all our divide-and-conquer trees, even with the taxonomic backbones, included unresolved nodes, which were particularly evident in species-rich clades where limited overlap in taxon sampling across subsets may have contributed to the increased number of polytomies. This suggests that the 50 subsets used for the divide-and-conquer analyses were insufficient and that additional subsets may be required to improve resolution, albeit at the cost of increased compute time.

Although the source trees differed between the supertree and divide-and-conquer analyses, both used the same approach to estimate the final tree and faced similar limitations. In both cases, the best results were achieved using taxonomic backbones. Although standardized taxonomic backbones are available for well-studied groups like birds, their absence in many other taxonomic groups limits the broader applicability of these methods. Even where these backbones are available, vastly different ranks may be used for clades of similar ages and species numbers in different parts of the Tree of Life. For example, there are 14,348 named ant species (Bolton 2025) and the ant crown group has an age of approximately 127 Ma (Borowiec et al. 2025), making the ants slightly more species-rich and older than birds. However, ants are classified as a family (Formicidae), rather than a class like birds, and this limits the number of taxonomic ranks that can be used for a supertree backbone or in assessment of clade recovery. Overall, these issues may limit the utility of supertree methods.

Identifying an appropriate weighting scheme for supertree methods is another challenge. The approach we used for our MRP gave a low weight for the backbone and assigned the largest weights to source trees based on the largest data sets, but it was ultimately ad hoc. Fortunately, the computational efficiency of supertree analyses allows for testing alternative weighting schemes (e.g., Moore et al. 2006; Baker et al. 2009; Nyakatura and Bininda-Emonds 2012) to evaluate their impact on resolution—provided robust criteria, such as expected clade recovery, are available for comparison. Finally, neither method inherently

supports branch length estimation. Various approaches can assign branch lengths to supertrees, with or without molecular data (e.g., Purvis 1995; Bininda-Emonds et al. 1999; Torices 2010; Kimball et al. 2019). In our study, branch length-optimized supertrees and divide-and-conquer trees yielded divergence time estimates that were similar to those from the concatenated trees, suggesting this limitation may not be critical for most studies.

Divergence Time Estimation

The timing of events in the avian phylogeny has been a topic of substantial debate. Some studies support an upper Cretaceous ancient origin for most high-level clades in Neoaves (Pacheco et al. 2011; Mitchell et al. 2015; Wu et al. 2024a, 2024b), while others suggest these lineages originated much closer to the Cretaceous-Paleogene (K-Pg) mass extinction event (~66 Ma) (Jarvis et al. 2014; Claramunt and Cracraft 2015; Prum et al. 2015; Kimball et al. 2019; Brocklehurst and Field 2024; Claramunt et al. 2024; Stiller et al. 2024). Despite these differences, all studies agree that crown birds originated in the mid- to late-Cretaceous, consistent with crown bird fossils predating the K-Pg boundary (e.g., Field et al. 2020).

Despite variation in tree topologies and branch lengths due to differences in data completeness, divergence time estimates were largely consistent across our methods (Fig. 7). This consistency held regardless of whether branch lengths were estimated during the tree search (RAxML-NG and fasttrees) or added later for methods that do not estimate meaningful branch lengths (supertree and divide-and-conquer analyses). These findings suggest that for downstream comparative analyses requiring time-calibrated trees, the choice of tree estimation method may have minimal impact, especially for deeper nodes, provided the method reliably recovers topological relationships. These results, supported by our calibrations, corroborate the hypothesis that the rapid diversification of modern birds occurred near the K-Pg event. Taking these factors into account, we present the first “macrophylogenomic tree” for birds, a resource that can be leveraged in future comparative research.

CONCLUSIONS

Overall, our analyses demonstrate that accurate macrophylogenies can be estimated using computationally efficient methods. This was achieved with a heterogeneous data set assembled from many independent studies, reflecting the likely approach for estimating most large-scale phylogenies across the Tree of Life. Although assembling such data sets introduces heterogeneity, our results demonstrate that filtering may not always be necessary. In fact, filtering can lead to lower accuracy, as we observed, where fewer expected clades

were recovered from filtered data sets compared with the full data set.

Our study employed the avian taxonomy from IOC v13.1 (2023) as the basis for the expected clades and the taxonomic backbones. This version provided a consistent and well-supported framework at the time of analysis. As ongoing research continues to refine our understanding of avian phylogenetics, more recent taxonomies can help resolve previously uncertain relationships. These updated resources can offer an even greater foundation for future studies, and our approach demonstrates the utility of a stable baseline for evaluating methodological performance.

Although we successfully estimated trees using several approaches that appeared accurate based on expected clade criterion, traditional supertree and divide-and-conquer methods required additional information, such as taxonomic backbones, to achieve results comparable to our best ML estimates. By contrast, our new fasttree approach with MP starting trees using the full data set provided a strong alternative to RAxML-NG, delivering similar topological accuracy and branch length estimates with a substantially reduced computational burden. Using this approach, replicate analyses to test different MP starting trees and models is also computationally efficient, and simple criteria, such as likelihood values, can be used to assess the resulting trees for those taxonomic groups that lack sufficient study to define expected clades. Thus, the new fasttree approach we used can be broadly applicable to any taxonomic group. By demonstrating the feasibility of computationally efficient methods, this study offers a roadmap for constructing large-scale phylogenies across the Tree of Life.

DATA AVAILABILITY

All the original data (accessions, alignments, summary statistics, taxon subsets, summary of all fasttree runs, clade ages, and tree files) and scripts necessary to reproduce the analyses reported in this study can be accessed through the Dryad link: <https://doi.org/10.5061/dryad.5dv41nsgw>.

DISCLAIMER

Any use of trade, firm, or product names is for descriptive purposes only and does not imply endorsement by the U.S. Government.

ACKNOWLEDGMENTS

We thank Bui Quang Minh for insights on the fasttree approach using IQ-TREE and Siavash Mirarab and Chao Zhang for advice on running large ASTRAL trees. We thank Jeremy Kirchman, Zongji Wang, and Qi Zhou for sharing tree files. We also thank J. Klicka, M. Ahmad, W. Tsai Nakashima, and E.M. Smith for support. Portions of this research were conducted with

high-performance computing resources provided by Louisiana State University (<http://www.hpc.lsu.edu>). For the purpose of open access, the authors have applied a Creative Commons Attribution (CC BY) license to any Author Accepted Manuscript version arising. We thank Bob Thomson, Marek Borowiec, and an anonymous reviewer for their valuable comments that improved this manuscript. We also thank Bob Thomson for relaying details of a discussion regarding the possible effects of differences in the resolution of taxonomic backbones on supertree methods that we incorporated to the text.

SUPPLEMENTARY MATERIAL

Data available from the Dryad Digital Repository: <https://doi.org/10.5061/dryad.5dv41nsgw>.

CONFLICT OF INTEREST

None declared.

FUNDING

This work was supported by National Science Foundation grant DEB-1655624 (B.C.F. and R.T.B.), DEB-2217442 (B.C.F. and R.T.B.—supplement), DEB-1655736 (B.T.S.), DEB-1655683 (E.L.B. and R.T.K.), DEB-2203216 (M.G.H., E.P.D., and R.T.B.), and Villum Fonden 25925 (P.A.H.). Part of this work was funded by UKRI grant MR/X015130/1.

REFERENCES

- Andermann T., Fernandes A.M., Olsson U., Töpel M., Pfeil B., Oxelman B., Aleixo A., Faircloth B.C., Antonelli A. 2019. Allele phasing greatly improves the phylogenetic utility of ultraconserved elements. *Syst. Biol.* 68:32–46. <https://doi.org/10.1093/sysbio/syy039>
- Andersen M.J., McCullough J.M., Friedman N.R., Peterson A.T., Moyle R.G., Joseph L., Nyári Á.S. 2019. Ultraconserved elements resolve genus-level relationships in a major Australasian bird radiation (Aves: Meliphagidae). *Emu* 119(3):218–232. <https://doi.org/10.1080/01584197.2019.1595662>
- Andersen M.J., McCullough J.M., Mauck W.M., Smith B.T., Moyle R.G. 2018. A phylogeny of kingfishers reveals an Indomalayan origin and elevated rates of diversification on oceanic islands. *J. Biogeogr.* 45(2):269–281. <https://doi.org/10.1111/jbi.13139>
- Bader D.A., Roshan U., Stamatakis A. 2006. Computational grand challenges in assembling the tree of life: problems and solutions. *Adv. Comput.* 68:127–176. [https://doi.org/10.1016/S0065-2458\(06\)68004-2](https://doi.org/10.1016/S0065-2458(06)68004-2)
- Baker W.J., Savolainen V., Asmussen-Lange C.B., Chase M.W., Dransfield J., Forest F., Harley M.M., Uhl N.W., Wilkinson M. 2009. Complete generic-level phylogenetic analyses of palms (Arecaceae) with comparisons of supertree and supermatrix approaches. *Syst. Biol.* 58(2):240–256. <https://doi.org/10.1093/sysbio/syp021>
- Baum B.R. 1992. Combining trees as a way of combining data sets for phylogenetic inference, and the desirability of combining gene trees. *Taxon* 41(1):3–10. <https://doi.org/10.2307/1222480>
- Bininda-Emonds O.R., Gittleman J.L., Purvis A. 1999. Building large trees by combining phylogenetic information: a complete phylogeny of the extant Carnivora (Mammalia). *Biol. Rev.* 74(2):143–175. <https://doi.org/10.1017/s0006323199005307>
- Bininda-Emonds O.R., Sanderson M.J. 2001. Assessment of the accuracy of matrix representation with parsimony analysis supertree construction. *Syst. Biol.* 50(4):565–579. <https://doi.org/10.1080/10635150120358>
- Bininda-Emonds O.R.P. 2004. The evolution of supertrees. *Trends Ecol. Evol.* 19(6):315–322. <https://doi.org/10.1016/j.tree.2004.03.015>
- Bininda-Emonds O.R.P., Gittleman J.L., Steel M.A. 2002. The (super)tree of life: procedures, problems, and prospects. *Annu. Rev. Ecol. Syst.* 33(1):265–289. <https://doi.org/10.1146/annurev.ecolsys.33.010802.150511>
- Bolton B. 2025. AntCat—an online catalog of the ants of the world. Available from: <https://antcat.org> (accessed 3 September 2025).
- Borowiec M.L. 2016. AMAS: a fast tool for alignment manipulation and computing of summary statistics. *PeerJ* 4:e1660. <https://doi.org/10.7717/peerj.1660>
- Borowiec M.L., Zhang Y.M., Neves K., Ramalho M.O., Fisher B.L., Lucky A., Moreau C.S. 2025. Evaluating UCE data adequacy and integrating uncertainty in a comprehensive phylogeny of ants. *Syst. Biol.* syaf001. <https://doi.org/10.1093/sysbio/syaf001>
- Braun E.L., Cracraft J., Houde P. 2019. Resolving the avian tree of life from top to bottom: the promise and potential boundaries of the phylogenomic era. In: Kraus R.H.S., editor. *Avian genomics in ecology and evolution: from the lab into the wild*. Cham: Springer International Publishing. p. 151–210. https://doi.org/10.1007/978-3-030-16477-5_6
- Braun E.L., Oliveros C.H., White Carreiro N.D., Zhao M., Glenn T.C., Brumfield R.T., Braun M.J., Kimball R.T., Faircloth B.C. 2024. Testing the mettle of METAL: a comparison of phylogenomic methods using a challenging but well-resolved phylogeny. *bioRxiv*. <https://doi.org/10.1101/2024.02.28.582627>
- Brocklehurst N., Field D.J. 2024. Tip dating and Bayes factors provide insight into the divergences of crown bird clades across the end-Cretaceous mass extinction. *Proc. R Soc. B* 291(2016):20232618. <https://doi.org/10.1098/rspb.2023.2618>
- Bruaux J., Gabrielli M., Ashari H., Prÿs-Jones R., Joseph L., Milá B., Besnard G., Thébaud C. 2018. Recovering the evolutionary history of crowned pigeons (Columbidae: Goura): implications for the biogeography and conservation of New Guinean lowland birds. *Mol. Phylogenet. Evol.* 120:248–258. <https://doi.org/10.1016/j.ympev.2017.11.022>
- Bryson R.W., Faircloth B.C., Tsai W.L.E., McCormack J.E., Klicka J. 2016. Target enrichment of thousands of ultraconserved elements sheds new light on early relationships within New World sparrows (Aves: Passerellidae). *Auk* 133(3):451–458. <https://doi.org/10.1642/AUK-16-26.1>
- Burga A., Wang W., Ben-David E., Wolf P.C., Ramey A.M., Verdugo C., Lyons K., Parker P.G., Kruglyak L. 2017. A genetic signature of the evolution of loss of flight in the Galapagos cormorant. *Science* 356(6341):eaal3345. <https://doi.org/10.1126/science.aal3345>
- Burleigh J.G., Kimball R.T., Braun E.L. 2015. Building the avian tree of life using a large-scale, sparse supermatrix. *Mol. Phylogenet. Evol.* 84:53–63. <https://doi.org/10.1016/j.ympev.2014.12.003>
- Campillo L.C., Oliveros C.H., Sheldon F.H., Moyle R.G. 2018. Genomic data resolve gene tree discordance in spiderhunters (Nectariniidae, *Arachnothera*). *Mol. Phylogenet. Evol.* 120:151–157. <https://doi.org/10.1016/j.ympev.2017.12.011>
- Capella-Gutiérrez S., Silla-Martínez J.M., Gabaldón T. 2009. trimAl: a tool for automated alignment trimming in large-scale phylogenetic analyses. *Bioinformatics* 25(15):1972–1973. <https://doi.org/10.1093/bioinformatics/btp348>
- Catanach T.A., Halley M.R., Allen J.M., Johnson J.A., Thorstrom R., Palhano S., Poor Thunder C., Gallardo J.C., Weckstein J.D. 2021. Systematics and conservation of an endemic radiation of Accipiter hawks in the Caribbean islands.

- Ornithology 138(3):ukab041. <https://doi.org/10.1093/ornithology/ukab041>
- Chen A., Field D.J. 2020. Phylogenetic definitions for Caprimulgiformes (Aves) and major constituent clades under the International Code of Phylogenetic Nomenclature. *Vertebr. Zool.* 70:571–585. <https://doi.org/10.26049/VZ70-4-2020-03>
- Chen D., Braun E.L., Forthman M., Kimball R.T., Zhang Z. 2018. A simple strategy for recovering ultraconserved elements, exons, and introns from low coverage shotgun sequencing of museum specimens: placement of the partridge genus *Tropicoperdix* within the Galliformes. *Mol. Phylogenet. Evol.* 129:304–314. <https://doi.org/10.1016/j.ympev.2018.09.005>
- Claramunt S., Braun E.L., Cracraft J., Fjeldså J., Ho S.Y.W., Houde P., Nguyen J.M.T., Stiller J. 2024. Calibrating the genomic clock of modern birds using fossils. *Proc. Natl. Acad. Sci. USA* 121(39):e2405887121. <https://doi.org/10.1073/pnas.2405887121>
- Claramunt S., Cracraft J. 2015. A new time tree reveals Earth history's imprint on the evolution of modern birds. *Sci. Adv.* 1(11):e1501005. <https://doi.org/10.1126/sciadv.1501005>
- Clements J.F., Rasmussen P.C., Schulenberg T.S., Iliff M.J., Fredericks T.A., Gerbracht J.A., Lepage D., Spencer A., Billerman S.M., Sullivan B.L., Wood C.L. 2023. The eBird/Clements checklist of Birds of the World: v2023. Available from: <https://www.birds.cornell.edu/clementschecklist/download/>
- Cotton J.A., Wilkin M. 2009. Supertrees join the mainstream of phylogenetics. *Trends Ecol. Evol.* 24(1):1–3. <https://doi.org/10.1016/j.tree.2008.08.006>
- Cracraft J., Donoghue M.J. 2004. *Assembling the tree of life*. Oxford, UK: Oxford University Press.
- Creevey C.J., McInerney J.O. 2005. Clann: investigating phylogenetic information through supertree analyses. *Bioinformatics* 21(3):390–392. <https://doi.org/10.1093/bioinformatics/bti020>
- de Queiroz K., Cantino P.D., Gauthier J.A., editors. 2020. *Phylogeny: A companion to the phylocode*. Boca Raton (FL): CRC Press.
- Delsuc F., Brinkmann H., Philippe H. 2005. Phylogenomics and the reconstruction of the tree of life. *Nat. Rev. Genet.* 6(5):361–375. <https://doi.org/10.1038/nrg1603>
- Dickinson EC, Christidis L, editors. 2014. *The Howard and Moore complete checklist of the birds of the world fourth edition*. Eastbourne: Aves Press.
- Driskell A.C., Ane C.e., Burleigh J.G., McMahon M.M., O'meara B.C., Sanderson M.J. 2004. Prospects for building the tree of life from large sequence databases. *Science* 306(5699):1172–1174. <https://doi.org/10.1126/science.1102036>
- Dwivedi B., Gadagkar S.R. 2009. Phylogenetic inference under varying proportions of indel-induced alignment gaps. *BMC Evol. Biol.* 9(1):211. <https://doi.org/10.1186/1471-2148-9-211>
- Everson K.M., McLaughlin J.F., Cato I.A., Evans M.M., Gastaldi A.R., Mills K.K., Shink K.G., Wilbur S.M., Winker K. 2019. Speciation, gene flow, and seasonal migration in *Catharus* thrushes (Aves: Turdidae). *Mol. Phylogenet. Evol.* 139:106564. <https://doi.org/10.1016/j.ympev.2019.106564>
- Faircloth B.C. 2016. PHYLUCES is a software package for the analysis of conserved genomic loci. *Bioinformatics* 32(5):786–788. <https://doi.org/10.1093/bioinformatics/btv646>
- Faircloth B.C., McCormack J.E., Crawford N.G., Harvey M.G., Brumfield R.T., Glenn T.C. 2012. Ultraconserved elements anchor thousands of genetic markers spanning multiple evolutionary timescales. *Syst. Biol.* 61(5):717–726. <https://doi.org/10.1093/sysbio/sys004>
- Felsenstein J. 1985. Confidence limits on phylogenies: an approach using the bootstrap. *Evolution* 39(4):783–791. <https://doi.org/10.2307/2408678>
- Ferreira M., Fernandes A.M., Aleixo A., Antonelli A., Olsson U., Bates J.M., Cracraft J., Ribas C.C. 2018. Evidence for mtDNA capture in the jacamar *Galbula leucogastra/chalcothorax* species-complex and insights on the evolution of white-sand ecosystems in the Amazon basin. *Mol. Phylogenet. Evol.* 129:149–157. <https://doi.org/10.1016/j.ympev.2018.07.007>
- Field D.J., Benito J., Chen A., Jagt J.W.M., Ksepka D.T. 2020. Late Cretaceous neornithine from Europe illuminates the origins of crown birds. *Nature* 579(7799):397–401. <https://doi.org/10.1038/s41586-020-2096-0>
- Gascuel O. 1997. BIONJ: an improved version of the NJ algorithm based on a simple model of sequence data. *Mol. Biol. Evol.* 14(7):685–695. <https://doi.org/10.1093/oxfordjournals.molbev.a025808>
- Gatesy J., Baker R.H., Hayashi C. 2004. Inconsistencies in arguments for the supertree approach: supermatrices versus supertrees of Crocodylia. *Syst. Biol.* 53(2):342–355. <https://doi.org/10.1080/10635150490423971>
- Gill F., Donsker D., Rasmussen P. 2023. IOC World Bird List (v 13.1). Available from: <http://dx.doi.org/10.14344/IOC.ML.13.1>
- Goloboff P.A., Catalano S.A., Marcos Mirande J., Szumik C.A., Salvador Arias J., Källersjö M., Farris J.S. 2009. Phylogenetic analysis of 73 060 taxa corroborates major eukaryotic groups. *Cladistics* 25(3):211–230. <https://doi.org/10.1111/j.1096-0031.2009.00255.x>
- Gu Z. 2022. Complex heatmap visualization. *iMeta* 1(3):e43. <https://doi.org/10.1002/imt2.43>
- Hackett S.J., Kimball R.T., Reddy S., Bowie R.C.K., Braun E.L., Braun M.J., Chojnowski J.L., Cox W.A., Han K.-L., Harshman J., Huddleston C.J., Marks B.D., Miglia K.J., Moore W.S., Sheldon F.H., Steadman D.W., Witt C.C., Yuri T. 2008. A phylogenomic study of birds reveals their evolutionary history. *Science* 320(5884):1763–1768. <https://doi.org/10.1126/science.1157704>
- Harvey M.G., Bravo G.A., Claramunt S., Cuervo A.M., Derryberry G.E., Battilana J., Seeholzer G.F., McKay J.S., O'meara B.C., Faircloth B.C., Edwards S.V., Pérez-Emán J., Moyle R.G., Sheldon F.H., Aleixo A., Smith B.T., Chesser R.T., Silveira L.F., Cracraft J., Brumfield R.T., Derryberry E.P. 2020. The evolution of a tropical biodiversity hotspot. *Science* 370(6522):1343–1348. <https://doi.org/10.1126/science.aaz6970>
- Hinchliff C.E., Smith S.A., Allman J.F., Burleigh J.G., Chaudhary R., Coghill L.M., Crandall K.A., Deng J., Drew B.T., Gazis R., Gude K., Hibbett D.S., Katz L.A., Laughinghouse H.D., McTavish E.J., Midford P.E., Owen C.L., Ree R.H., Rees J.A., Soltis D.E., Williams T., Cranston K.A. 2015. Synthesis of phylogeny and taxonomy into a comprehensive tree of life. *Proc. Natl. Acad. Sci. USA* 112(41):12764–12769. <https://doi.org/10.1073/pnas.1423041112>
- Hosner P.A., Faircloth B.C., Glenn T.C., Braun E.L., Kimball R.T. 2016. Avoiding missing data biases in phylogenomic inference: an empirical study in the landfowl (Aves: Galliformes). *Mol. Biol. Evol.* 33(4):1110–1125. <https://doi.org/10.1093/molbev/msv347>
- Huerta-Cepas J., Serra F., Bork P. 2016. ETE 3: reconstruction, analysis, and visualization of phylogenomic data. *Mol. Biol. Evol.* 33(6):1635–1638. <https://doi.org/10.1093/molbev/msw046>
- Imfeld T.S., Barker F.K., Brumfield R.T. 2020. Mitochondrial genomes and thousands of ultraconserved elements resolve the taxonomy and historical biogeography of the *Euphonia* and *Chlorophonia* finches (Passeriformes: Fringillidae). *Auk* 137(3):ukaa016. <https://doi.org/10.1093/auk/ukaa016>
- Jarvis E.D., Mirarab S., Aberer A.J., Li B., Houde P., Li C., Ho S.Y.W., Faircloth B.C., Nabolz B., Howard J.T., Suh A., Weber C.C., DeFonseca R.R., Li J., Zhang F., Li H., Zhou L., Narula N., Liu L., Ganapathy G., Boussau B., Md Bayzid S., Zavidovych V., Subramanian S., Gabaldón T., Capella-Gutiérrez S., Huerta-Cepas J., Rekepalli B., Munch K., Schierup M., Lindov B., Warren W.C., Ray D., Green R.E., Zhang G., Bruford M.W., Zhan X., Dixon A., Li S., Li N., Huang Y., Derryberry E.P., Bertelsen M.F., Sheldon F.H., Brumfield R.T., Mello C.V., Lovell P.V., Wirthlin M., Schneider M.P., Prosdociimi F., Samaniego J.A., Vargas Velazquez A.M., Alfaro-Núñez A., Campos P.F., Petersen B., Sicheritz-Ponten T., Pas A., Bailey T., Scofield P., Bunce M., Lambert D.M., Zhou Q., Perelman P., Driskell A.C., Shapiro B., Xiong Z., Zeng Y., Liu S., Li Z., Liu B., Wu K., Xiao J., Yinqi X., Zheng Q., Zhang Y., Yang H., Wang J., Smeds L., Rheindt F.E., Braun M., Fjeldsa J., Orlando L., Barker F.K., Jönsson K.A., Johnson W., Koepfli K.P., O'Brien S., Haussler D., Ryder O.A., Rahbek C., Willerslev E., Graves G.R., Glenn T.C., McCormack J., Burt D., Ellegren H., Alström P., Edwards S.V., Stamatakis A., Mindell

- D.P., Cracraft J., Braun E.L., Warnow T., Jun W., Gilbert M.T., 2014. Whole-genome analyses resolve early branches in the tree of life of modern birds. *Science* 346(6215):1320–1331. <https://doi.org/10.1126/science.1253451>
- Jetz W., Thomas G.H., Joy J.B., Hartmann K., Mooers A.O. 2012. The global diversity of birds in space and time. *Nature* 491(7424):444–448. <https://doi.org/10.1038/nature11631>
- Kapli P., Yang Z., Telford M.J. 2020. Phylogenetic tree building in the genomic age. *Nat. Rev. Genet.* 21(7):428–444. <https://doi.org/10.1038/s41576-020-0233-0>
- Katoh K., Standley D.M. 2013. MAFFT multiple sequence alignment software version 7: improvements in performance and usability. *Mol. Biol. Evol.* 30(4):772–780. <https://doi.org/10.1093/molbev/mst010>
- Kimball R.T., Braun E.L., Barker F.K., Bowie R.C.K., Braun M.J., Chojnowski J.L., Hackett S.J., Han K.-L., Harshman J., Heimer-Torres V. 2009. A well-tested set of primers to amplify regions spread across the avian genome. *Mol. Phylogenet. Evol.* 50(3):654–660. <https://doi.org/10.1016/j.ympev.2008.11.018>
- Kimball R.T., Oliveros C.H., Wang N., White N.D., Barker F.K., Field D.J., Ksepka D.T., Chesser R.T., Moyle R.G., Braun M.J., Brumfield R.T., Faircloth B.C., Smith B.T., Braun E.L. 2019. A phylogenomic super-tree of birds. *Diversity* 11(7):109. <https://doi.org/10.3390/d11070109>
- Kirchman J.J., Rotzel McInerney N., Giarla T.C., Olson S.L., Slikas E., Fleischer R.C. 2021. Phylogeny based on ultra-conserved elements clarifies the evolution of rails and allies (Ralloidea) and is the basis for a revised classification. *Ornithology* 138(4):ukab042. <https://doi.org/10.1093/ornithology/ukab042>
- Koonin E.V. 2005. Orthologs, paralogs, and evolutionary genomics. *Annu. Rev. Genet.* 39(1):309–338. <https://doi.org/10.1146/annurev.genet.39.073003.114725>
- Kozlov A.M., Darriba D., Flouri T., Morel B., Stamatakis A. 2019. RAxML-NG: a fast, scalable and user-friendly tool for maximum likelihood phylogenetic inference. *Bioinformatics* 35(21):4453–4455. <https://doi.org/10.1093/bioinformatics/btz305>
- Kuhl H., Frankl-Vilches C., Bakker A., Mayr G., Nikolaus G., Boerno S.T., Klages S., Timmermann B., Gahr M. 2021. An unbiased molecular approach using 3'-UTRs resolves the avian family-level tree of life. *Mol. Biol. Evol.* 38(1):108–127. <https://doi.org/10.1093/molbev/msaa191>
- Lamichhane S., Berglund J., Almén M.S., Maqbool K., Grabherr M., Martínez-Barrio A., Promerová M., Rubín C.-J., Wang C., Zamani N., Grant B.R., Grant P.R., Webster M.T., Andersson L. 2015. Evolution of Darwin's finches and their beaks revealed by genome sequencing. *Nature* 518(7539):371–375. <https://doi.org/10.1038/nature14181>
- Lê S., Josse J., Husson F. 2008. FactoMineR: an R package for multivariate analysis. *J. Stat. Soft.* 25(1):1–18. <https://doi.org/10.18637/jss.v025.i01>
- Leite R.N., Kimball R.T., Braun E.L., Derryberry E.P., Hosner P.A., Derryberry G.E., Anciães M., McKay J.S., Aleixo A., Ribas C.C., Brumfield R.T., Cracraft J. 2021. Phylogenomics of manakins (Aves: Pipridae) using alternative locus filtering strategies based on informativeness. *Mol. Phylogenet. Evol.* 155:107013. <https://doi.org/10.1016/j.ympev.2020.107013>
- Liu F.G., Miyamoto M.M., Freire N.P., Ong P.Q., Tennant M.R., Young T.S., Gugel K.F. 2001. Molecular and morphological supertrees for eutherian (placental) mammals. *Science* 291(5509):1786–1789. <https://doi.org/10.1126/science.1056346>
- Liu L., Yu L., Edwards S.V. 2010. A maximum pseudo-likelihood approach for estimating species trees under the coalescent model. *BMC Evol. Biol.* 10(1):302. <https://doi.org/10.1186/1471-2148-10-302>
- McCormack J.E., Harvey M.G., Faircloth B.C., Crawford N.G., Glenn T.C., Brumfield R.T. 2013. A phylogeny of birds based on over 1,500 loci collected by target enrichment and high-throughput sequencing. *PLoS One* 8(1):e54848. <https://doi.org/10.1371/journal.pone.0054848>
- McCormack J.E., Hird S.M., Zellmer A.J., Carstens B.C., Brumfield R.T. 2013. Applications of next-generation sequencing to phylogeography and phylogenetics. *Mol. Phylogenet. Evol.* 66(2):526–538. <https://doi.org/10.1016/j.ympev.2011.12.007>
- McCormack J.E., Tsai W.L.E., Faircloth B.C. 2016. Sequence capture of ultraconserved elements from bird museum specimens. *Mol. Ecol. Resour.* 16(5):1189–1203. <https://doi.org/10.1111/1755-0998.12466>
- McCullough J.M., Joseph L., Moyle R.G., Andersen M.J. 2019. Ultraconserved elements put the final nail in the coffin of traditional use of the genus *Meliphaga* (Aves: Meliphagidae). *Zoologica Scripta* 48(4):411–418. <https://doi.org/10.1111/zsc.12350>
- McCullough J.M., Moyle R.G., Smith B.T., Andersen M.J. 2019. A Laurasian origin for a pantropical bird radiation is supported by genomic and fossil data (Aves: Coraciiformes). *Proc. R. Soc. B* 286(1910):20190122. <https://doi.org/10.1098/rspb.2019.0122>
- McCullough J.M., Oliveros C.H., Benz B.W., Zenil-Ferguson R., Cracraft J., Moyle R.G., Andersen M.J. 2022. Wallacean and Melanesian Islands Promote higher rates of diversification within the global passerine radiation Corvidae. *Syst. Biol.* 71(6):1423–1439. <https://doi.org/10.1093/sysbio/syaa044>
- Mctavish E.J., Gerbracht J.A., Holder M.T., Iliff M.J., Lepage D., Rasmussen P.C., Redelings B.D., Sánchez Reyes L.L., Miller E.T. 2024. A complete and dynamic tree of birds. *Proc. Natl. Acad. Sci. USA* 122(18):e2409658122. <https://doi.org/10.1073/pnas.2409658122>
- Manthey J.D., Campillo L.C., Burns K.J., Moyle R.G. 2016. Comparison of target-capture and restriction-site associated DNA sequencing for phylogenomics: a test in Cardinalid Tanagers (Aves, Genus: *Piranga*). *Syst. Biol.* 65(4):640–650. <https://doi.org/10.1093/sysbio/syw005>
- Minh B.Q., Schmidt H.A., Chernomor O., Schrempf D., Woodhams M.D., von Haeseler A., Lanfear R. 2020. IQ-TREE 2: new models and efficient methods for phylogenetic inference in the genomic era. *Mol. Biol. Evol.* 37(5):1530–1534. <https://doi.org/10.1093/molbev/msa015>
- Mitchell K.J., Cooper A., Phillips M.J. 2015. Comment on “whole-genome analyses resolve early branches in the tree of life of modern birds”. *Science* 349(6255):1460. <https://doi.org/10.1126/science.aa01062>
- Moore B., Smith S., Donoghue M. 2006. Increasing data transparency and estimating phylogenetic uncertainty in supertrees: approaches using nonparametric bootstrapping. *Syst. Biol.* 55(4):662–676. <https://doi.org/10.1080/1063515060920693>
- Moyle R.G., Oliveros C.H., Andersen M.J., Hosner P.A., Benz B.W., Manthey J.D., Travers S.L., Brown R.M., Faircloth B.C. 2016. Tectonic collision and uplift of Wallacea triggered the global songbird radiation. *Nat. Commun.* 7(1):12709. <https://doi.org/10.1038/ncomms12709>
- Musher L.J., Cracraft J. 2018. Phylogenomics and species delimitation of a complex radiation of Neotropical suboscine birds (*Pachyrhamphus*). *Mol. Phylogenet. Evol.* 118:204–221. <https://doi.org/10.1016/j.ympev.2017.09.013>
- Nater A., Burri R., Kawakami T., Smeds L., Ellegren H. 2015. Resolving evolutionary relationships in closely related species with whole-genome sequencing data. *Syst. Biol.* 64(6):1000–1017. <https://doi.org/10.1093/sysbio/syv045>
- Nguyen L.-T., Schmidt H.A., von Haeseler A., Minh B.Q. 2015. IQ-TREE: a fast and effective stochastic algorithm for estimating maximum-likelihood phylogenies. *Mol. Biol. Evol.* 32(1):268–274. <https://doi.org/10.1093/molbev/msu300>
- Nixon K. 1999. The parsimony ratchet, a new method for rapid parsimony analysis. *Cladistics* 15(4):407–414. <https://doi.org/10.1111/j.1096-0031.1999.tb00277.x>
- Nyakatura K., Bininda-Emonds O.R.P. 2012. Updating the evolutionary history of Carnivora (Mammalia): a new species-level supertree complete with divergence time estimates. *BMC Biol.* 10(1):12. <https://doi.org/10.1186/1741-7007-10-12>
- Ogden T.H., Rosenberg M.S. 2006. Multiple sequence alignment accuracy and phylogenetic inference.

- Syst. Biol. 55(2):314–328. <https://doi.org/10.1080/10635150500541730>
- Oliveros C.H., Andersen M.J., Hosner P.A., Mauck W.M., Sheldon F.H., Cracraft J., Moyle R.G. 2020. Rapid Laurasian diversification of a pantropical bird family during the Oligocene–Miocene transition. *Ibis* 162(1):137–152. <https://doi.org/10.1111/ibi.12707>
- Oliveros C.H., Andersen M.J., Moyle R.G. 2021. A phylogeny of white-eyes based on ultraconserved elements. *Mol. Phylogenet. Evol.* 164:107273. <https://doi.org/10.1016/j.ympev.2021.107273>
- Oliveros C.H., Field D.J., Ksepka D.T., Barker F.K., Aleixo A., Andersen M.J., Alström P., Benz B.W., Braun E.L., Braun M.J., Bravo G.A., Brumfield R.T., Chesser R.T., Claramunt S., Cracraft J., Cuervo A.M., Derryberry E.P., Glenn T.C., Harvey M.G., Faircloth B.C., Hosner P.A., Joseph L., Kimball R.T., Mack A.L., Miskelly C.M., Peterson A.T., Robbins M.B., Sheldon F.H., Silveira L.F., Smith B.T., White N.D., Moyle R.G., 2019. Earth history and the passerine superradiation. *Proc. Natl. Acad. Sci. USA* 116(16):7916–7925. <https://doi.org/10.1073/pnas.1813206116>
- Ottenburghs J., Megens H.-J., Kraus R.H.S., Madsen O., van Hooft P., van Wieren S.E., Crooijmans R., Ydenberg R.C., Groenen M.A.M., Prins H.H.T. 2016. A tree of geese: a phylogenomic perspective on the evolutionary history of True Geese. *Mol. Phylogenet. Evol.* 101:303–313. <https://doi.org/10.1016/j.ympev.2016.05.021>
- Pacheco M.A., Battistuzzi F.U., Lentino M., Aguilar R.F., Kumar S., Escalante A.A. 2011. Evolution of modern birds revealed by mitogenomics: timing the radiation and origin of major orders. *Mol. Biol. Evol.* 28(6):1927–1942. <https://doi.org/10.1093/molbev/msr014>
- Paradis E., Schliep K. 2019. ape 5.0: an environment for modern phylogenetics and evolutionary analyses in R. *Bioinformatics* 35(3):526–528. <https://doi.org/10.1093/bioinformatics/bty633>
- Parham J.F., Donoghue P.C.J., Bell C.J., Calway T.D., Head J.J., Holroyd P.A., Inoue J.G., Irmis R.B., Joyce W.G., Ksepka D.T., Patané J.S.L., Smith N.D., Tarver J.E., van Tuinen M., Yang Z., Angielczyk K.D., Greenwood J.M., Hipsley C.A., Jacobs L., Benton M.J., Makovicky P.J., Müller J., Smith K.T., Theodor J.M., Warnock R.C., 2012. Best practices for justifying fossil calibrations. *Syst. Biol.* 61(2):346–359. <https://doi.org/10.1093/sysbio/syr107>
- Philippe H., Brinkmann H., Lavrov D.V., Littlewood D.T.J., Manuel M., Wörheide G., Baurain D. 2011. Resolving difficult phylogenetic questions: why more sequences are not enough. *PLoS Biol.* 9(3):e1000602. <https://doi.org/10.1371/journal.pbio.1000602>
- Philippe H., Snell E.A., Baptiste E., Lopez P., Holland P.W.H., Casane D. 2004. Phylogenomics of eukaryotes: impact of missing data on large alignments. *Mol. Biol. Evol.* 21(9):1740–1752. <https://doi.org/10.1093/molbev/msh182>
- Portik D.M., Wiens J.J. 2021. Do alignment and trimming methods matter for phylogenomic (UCE) analyses? *Syst. Biol.* 70(3):440–462. <https://doi.org/10.1093/sysbio/syaa064>
- Price M.N., Dehal P.S., Arkin A.P. 2010. FastTree 2—approximately maximum-likelihood trees for large alignments. *PLoS One* 5(3):e9490. <https://doi.org/10.1371/journal.pone.0009490>
- Prum R.O., Berv J.S., Dornburg A., Field D.J., Townsend J.P., Lemmon E.M., Lemmon A.R. 2015. A comprehensive phylogeny of birds (Aves) using targeted next-generation DNA sequencing. *Nature* 526(7574):569–573. <https://doi.org/10.1038/nature15697>
- Purvis A. 1995. A composite estimate of primate phylogeny. *Phil. Trans. R. Soc. Lond. B* 348(1326):405–421. <https://doi.org/10.1098/rstb.1995.0078>
- R Core Team. 2023. R: A language and environment for statistical computing. Vienna: R Foundation for Statistical Computing
- Ragan M.A. 1992. Phylogenetic inference based on matrix representation of trees. *Mol. Phylogenet. Evol.* 1(1):53–58. [https://doi.org/10.1016/1055-7903\(92\)90035-F](https://doi.org/10.1016/1055-7903(92)90035-F)
- Reddy S., Kimball R.T., Pandey A., Hosner P.A., Braun M.J., Hackett S.J., Han K.-L., Harshman J., Huddleston C.J., Kingston S., Marks B.D., Miglia K.J., Moore W.S., Sheldon F.H., Witt C.C., Yuri T., Braun E.L. 2017. Why do phylogenomic data sets yield conflicting trees? Data type influences the avian tree of life more than taxon sampling. *Syst. Biol.* 66(5):857–879. <https://doi.org/10.1093/sysbio/syx041>
- Redelings B.D., Holder M.T. 2017. A supertree pipeline for summarizing phylogenetic and taxonomic information for millions of species. *PeerJ* 5:e3058. <https://doi.org/10.7717/peerj.3058>
- Robinson D.F., Foulds L.R. 1981. Comparison of phylogenetic trees. *Math. Biosci.* 53(1–2):131–147. [https://doi.org/10.1016/0025-5564\(81\)90043-2](https://doi.org/10.1016/0025-5564(81)90043-2)
- Sackton T.B., Grayson P., Cloutier A., Hu Z., Liu J.S., Wheeler N.E., Gardner P.P., Clarke J.A., Baker A.J., Clamp M., Edwards S.V. 2019. Convergent regulatory evolution and loss of flight in paleognathous birds. *Science* 364(6435):74–78. <https://doi.org/10.1126/science.aat7244>
- Salter J.F., Oliveros C.H., Hosner P.A., Manthey J.D., Robbins M.B., Moyle R.G., Brumfield R.T., Faircloth B.C. 2020. Extensive paraphyly in the typical owl family (Strigidae). *Auk* 137(1):ukz070. <https://doi.org/10.1093/auk/ukz070>
- Sanderson M.J., McMahon M.M., Steel M. 2010. Phylogenomics with incomplete taxon coverage: the limits to inference. *BMC Evol. Biol.* 10(1):155. <https://doi.org/10.1186/1471-2148-10-155>
- Sanderson M.J., Purvis A., Henze C. 1998. Phylogenetic supertrees: assembling the trees of life. *Trends Ecol. Evol.* 13(3):105–109. [https://doi.org/10.1016/S0169-5347\(97\)01242-1](https://doi.org/10.1016/S0169-5347(97)01242-1)
- Sangster G., Braun E.L., Johansson U.S., Kimball R.T., Mayr G., Suh A. 2022. Phylogenetic definitions for 25 higher-level clade names of birds. *Avian Res.* 13:100027. <https://doi.org/10.1016/j.avrs.2022.100027>
- Sangster G., Mayr G. 2021. Feraequornithes: a name for the clade formed by Procellariiformes, Sphenisciformes, Ciconiiformes, Suliformes and Pelecaniformes (Aves). *VZ* 71:49–53. <https://doi.org/10.3897/vz.71.e61728>
- Schliep K.P. 2011. phangorn: phylogenetic analysis in R. *Bioinformatics* 27(4):592–593. <https://doi.org/10.1093/bioinformatics/btq706>
- Schwery O., O'Meara B.C. 2016. MonoPhy: a simple R package to find and visualize monophyly issues. *PeerJ Comput. Sci.* 2:e56. <https://doi.org/10.7717/peerj-cs.56>
- Smith B.T., Harvey M.G., Faircloth B.C., Glenn T.C., Brumfield R.T. 2014. Target capture and massively parallel sequencing of ultraconserved elements for comparative studies at shallow evolutionary time scales. *Syst. Biol.* 63(1):83–95. <https://doi.org/10.1093/sysbio/syt061>
- Smith B.T., Mauck W.M., Benz B.W., Andersen M.J. 2020. Uneven missing data skew phylogenomic relationships within the Lories and Lorikeets. *Genome Biol. Evol.* 12(7):1131–1147. <https://doi.org/10.1093/gbe/evaa113>
- Smith B.T., Merwin J., Provost K.L., Thom G., Brumfield R.T., Ferreira M., Mauck W.M., Moyle R.G., Wright T.F., Joseph L. 2023. Phylogenomic analysis of the parrots of the world distinguishes artifactual from biological sources of gene tree discordance. *Syst. Biol.* 72(1):228–241. <https://doi.org/10.1093/sysbio/syaa055>
- Smith S.A., O'Meara B.C. 2012. treePL: divergence time estimation using penalized likelihood for large phylogenies. *Bioinformatics* 28(20):2689–2690. <https://doi.org/10.1093/bioinformatics/bts492>
- Springer M.S., Gatesy J. 2014. Land plant origins and coalescence confusion. *Trends Plant Sci.* 19(5):267–269. <https://doi.org/10.1016/j.tplants.2014.02.012>
- Stiller J., Feng S., Chowdhury A.A., Rivas-González I., Duchêne D.A., Fang Q., Deng Y., Kozlov A., Stamatakis A., Claramunt S., Nguyen J.M.T., Ho S.Y.W., Faircloth B.C., Haag J., Houde P., Cracraft J., Balaban M., Mai U., Chen G., Zhang G., Gao R., Zhou C., Xie Y., Huang Z., Cao Z., Yan Z., Ogilvie H.A., Nakhleh L., Lindow B., Morel B., Fjeldså J., Hosner P.A., da Fonseca R.R., Petersen B., Tobias J.A., Székely T., Kennedy J.D., Reeve A.H., Liker A., Stervander M., Antunes A., Tietze D.T., Bertelsen M.F., Lei F., Rahbek C., Graves G.R., Schierup M.H., Warnow T., Braun E.L., Gilbert M.T.P., Jarvis E.D., Mirarab S., 2024. Complexity of avian evolution revealed by family-level genomes. *Nature* 629(8013):851–860. <https://doi.org/10.1038/s41586-024-07323-1>
- Sukumaran J., Holder M.T. 2010. DendroPy: a Python library for phylogenetic computing. *Bioinformatics* 26(12):1569–1571.

- Sun K., Meiklejohn K.A., Faircloth B.C., Glenn T.C., Braun E.L., Kimball R.T. 2014. The evolution of peafowl and other taxa with ocelli (eye-spots): a phylogenomic approach. *Proc. R Soc. B* 281(1790):20140823. <https://doi.org/10.1098/rspb.2014.0823>
- Swofford D.L. 2003. PAUP* Phylogenetic Analysis Using Parsimony (*and other methods). Version 4. Available from: <http://paup.csit.fsu.edu/>
- Tan G., Muffato M., Ledergerber C., Herrero J., Goldman N., Gil M., Dessimoz C. 2015. Current methods for automated filtering of multiple sequence alignments frequently used single-gene phylogenetic inference. *Syst. Biol.* 64(5):778–791. <https://doi.org/10.1093/sysbio/syv033>
- Title P.O., Rabosky D.L. 2017. Do macrophylogenies yield stable macroevolutionary inferences? An example from squamate reptiles. *Syst. Biol.* 66:843–856. <https://doi.org/10.1093/sysbio/syw102>
- Togkousidis A., Stamatakis A., Gascuel O. 2025. Accelerating maximum likelihood phylogenetic inference via early stopping to evade (over-)optimization. *Syst. Biol.* syaf043. <https://doi.org/10.1093/sysbio/syaf043>
- Torices R. 2010. Adding time-calibrated branch lengths to the Asteraceae supertree. *J. Syst. Evol.* 48(4):271–278. <https://doi.org/10.1111/j.1759-6831.2010.00088.x>
- Vianna J.A., Fernandes F.A.N., Frugone M.J., Figueiró H.V., Pertierra L.R., Noll D., Bi K., Wang-Claypool C.Y., Lowther A., Parker P., Le Bohec C., Bonadonna F., Wienecke B., Pistorius P., Steinfurth A., Burridge C.P., Dantas G.P.M., Poulin E., Simison W.B., Bowie R.C.K., Henderson J., Eizirik E., Nery M.F., 2020. Genome-wide analyses reveal drivers of penguin diversification. *Proc. Natl. Acad. Sci. USA* 117(36):22303–22310. <https://doi.org/10.1073/pnas.2006659117>
- Vinay K.L., Natesh M., Mehta P., Jayapal R., Mukherjee S., Robin V.V. 2022. Re-assessing the phylogenetic status and evolutionary relationship of Forest Owllet (*Athene blewitti* (Hume 1873)) using genomic data. *Ibis* 164(4):1278–1284. <https://doi.org/10.1111/ibi.13097>
- Wang N., Hosner P.A., Liang B., Braun E.L., Kimball R.T. 2017. Historical relationships of three enigmatic phasianid genera (Aves: galliformes) inferred using phylogenomic and mitogenomic data. *Mol. Phylogenet. Evol.* 109:217–225. <https://doi.org/10.1016/j.ympev.2017.01.006>
- Wang Z., Zhang J., Xu X., Witt C., Deng Y., Chen G., Meng G., Feng S., Xu L., Szekely T., Zhang G., Zhou Q. 2022. Phylogeny and sex chromosome evolution of Palaeognathae. *J. Genet. Genom.* 49(2):109–119. <https://doi.org/10.1016/j.jgg.2021.06.013>
- White N.D., Braun M.J. 2019. Extracting phylogenetic signal from phylogenomic data: higher-level relationships of the nightbirds (Strisores). *Mol. Phylogenet. Evol.* 141:106611. <https://doi.org/10.1016/j.ympev.2019.106611>
- White N.D., Mitter C., Braun M.J. 2017. Ultraconserved elements resolve the phylogeny of potoos (Aves: Nyctibiidae). *J. Avian Biol.* 48(6):872–880. <https://doi.org/10.1111/jav.01313>
- Wickham H. 2011. ggplot2. *WIREs Comp. Stat.* 3(2):180–185. <https://doi.org/10.1002/wics.147>
- Wilkinson M., Pisani D., Cotton J.A., Corfe I. 2005. Measuring support and finding unsupported relationships in supertrees. *Syst. Biol.* 54(5):823–831. <https://doi.org/10.1080/10635150590950362>
- Winker K., Glenn T.C., Faircloth B.C. 2018. Ultraconserved elements (UCEs) illuminate the population genomics of a recent, high-latitude avian speciation event. *PeerJ* 6:e5735. <https://doi.org/10.7717/peerj.5735>
- Wu S., Rheindt F.E., Zhang J., Wang J., Zhang L., Quan C., Li Z., Wang M., Wu F., Qu Y., Edwards S.V., Zhou Z., Liu L. 2024a. Genomes, fossils, and the concurrent rise of modern birds and flowering plants in the Late Cretaceous. *Proc. Natl. Acad. Sci. USA* 121(8):e2319696121. <https://doi.org/10.1073/pnas.2319696121>
- Wu S., Rheindt F.E., Zhang J., Wang J., Zhang L., Quan C., Li Z., Wang M., Wu F., Qu Y., Edwards S.V., Zhou Z., Liu L. 2024b. Reply to Claramunt: robustness of the Cretaceous radiation of crown aves. *Proc. Natl. Acad. Sci. USA* 121(39):e2412448121. <https://doi.org/10.1073/pnas.2412448121>
- Xi Z., Liu L., Davis C.C. 2016. The impact of missing data on species tree estimation. *Mol. Biol. Evol.* 33(3):838–860. <https://doi.org/10.1093/molbev/msv266>
- Yang Z., Rannala B. 2012. Molecular phylogenetics: principles and practice. *Nat. Rev. Genet.* 13(5):303–314. <https://doi.org/10.1038/nrg3186>
- Yonezawa T., Segawa T., Mori H., Campos P.F., Hongoh Y., Endo H., Akiyoshi A., Kohno N., Nishida S., Wu J., Jin H., Adachi J., Kishino H., Kurokawa K., Nogi Y., Tanabe H., Mukoyama H., Yoshida K., Rasoamiamanana A., Yamagishi S., Hayashi Y., Yoshida A., Koike H., Akishinomiya F., Willerslev E., Hasegawa M. 2017. Phylogenomics and morphology of extinct paleognaths reveal the origin and evolution of the ratites. *Curr. Biol.* 27(1):68–77. <https://doi.org/10.1016/j.cub.2016.10.029>
- Younger J.L., Strozier L., Maddox J.D., Nyári Á.S., Bonfitto M.T., Raherilao M.J., Goodman S.M., Reddy S. 2018. Hidden diversity of forest birds in Madagascar revealed using integrative taxonomy. *Mol. Phylogenet. Evol.* 124:16–26. <https://doi.org/10.1016/j.ympev.2018.02.017>
- Zarza E., Faircloth B.C., Tsai W.L.E., Bryson R.W., Klicka J., McCormack J.E. 2016. Hidden histories of gene flow in highland birds revealed with genomic markers. *Mol. Ecol.* 25(20):5144–5157. <https://doi.org/10.1111/mec.13813>
- Zhang C., Rabiee M., Sayyari E., Mirarab S. 2018. ASTRAL-III: polynomial time species tree reconstruction from partially resolved gene trees. *BMC Bioinf.* 19(S6):153. <https://doi.org/10.1186/s12859-018-2129-y>
- Zhang G., Li B., Li C., Gilbert M.T.P., Jarvis E.D., Wang J., Avian Genome Consortium. 2014. Comparative genomic data of the Avian Phylogenomics Project. *GigaScience* 3(1):26. <https://doi.org/10.1186/2047-217X-3-26>
- Zhao M., Kurtis S.M., White N.D., Moncrieff A.E., Leite R.N., Brumfield R.T., Braun E.L., Kimball R.T. 2023. Exploring conflicts in whole genome phylogenetics: a case study within manakins (Aves: pipridae). *Syst. Biol.* 72(1):161–178. <https://doi.org/10.1093/sysbio/syaa062>
- Zhao M., Oswald J.A., Allen J.M., Owens H.L., Hosner P.A., Guralnick R.P., Braun E.L., Kimball R.T. 2025. A phylogenomic tree of wood-warblers (Aves: Parulidae): dealing with good, bad, and ugly samples. *Mol. Phylogenet. Evol.* 202:108235. <https://doi.org/10.1016/j.ympev.2024.108235>